Regulation of Myoplasmic Ca^{2+} During Fatigue in K_{ATP} Channel Deficient FDB Muscle Fibres

By

David Selvin

A thesis submitted to the Faculty of Graduate and Post-Doctoral Studies
of the University of Ottawa
in partial fulfillment of the requirements
of the Degree of **Masters of Science**

Department of Cellular and Molecular Medicine
Faculty of Medicine
University of Ottawa

ABSTRACT

It is known that muscles that lack K_{ATP} channel activity generate much greater unstimulated $[Ca^{2+}]_i$ and force than normal muscles during fatigue. The increase in unstimulated force in K_{ATP} channel deficient muscles is abolished by a partial inhibition of L-type Ca^{2+} channels, suggesting that it is due to a Ca^{2+} influx through L-type Ca^{2+} channels and a subsequent increased myoplasmic Ca^{2+}. However, there is also evidence that the increase in resting force is abolished by NAC, a ROS scavenger. The objective of this study was to reconcile these observations by studying the hypothesis that "the increase in resting $[Ca^{2+}]_i$ during fatigue in K_{ATP} channel deficient muscles starts with an excess Ca^{2+} influx through L-type Ca^{2+} channels, followed by an excess ROS production that causes a further increase in resting $[Ca^{2+}]_i$". To test the hypothesis, single FDB fibres were fatigued with one tetanic contraction/sec for 180 sec. K_{ATP} channel deficient fibres were obtained i) by exposing wild type muscle fibers to glibenclamide, a K_{ATP} channel blocker and ii) by using fibres from Kir6.2$^{-/-}$ mice, which are null mice for the Kir6.2 gene that encodes for the protein forming the channel pore. Verapamil, a L-type Ca^{2+} channel blocker, applied at 1 μM, significantly reduced resting $[Ca^{2+}]_i$ during fatigue in glibenclamide-exposed wild type fibres. NAC (1 mM) also reduced resting $[Ca^{2+}]_i$ in glibenclamide-exposed muscles. The results suggest that the increase in resting $[Ca^{2+}]_i$ during fatigue in K_{ATP} channel deficient FDB fibres is due to an influx through L-type Ca^{2+} channels, and an excess ROS production.

ABBREVIATIONS

$[ATP]_i$	Intracellular adenosine triphosphate concentration
$[Ca^{2+}]_i$	Intracellular calcium concentration
$[K^+]_i$	Intracellular potassium concentration
$[Na^+]_i$	Intracellular sodium concentration
ACh	Acetylcholine
ADP	Adenosine diphosphate
AMP	Adenosine monophosphate
AP	Action potential
ATP	Adenosine triphosphate
Ca^{2+}	Calcium ion
Ca_v	Voltage-gated calcium channel
ClC	Chloride channel
CNS	Central nervous system
DHPR	Dihydropyridine receptor
E_m	Membrane potential
G_k	Potassium conductance
G_{Na}	Sodium conductance
IMP	Inosine monophosphate
K^+	Potassium ion
K_{ATP} Channel	Adenosine triphosphate-sensitive potassium channel
Kir	Inward-rectifying potassium channel
Na^+	Sodium ion

NAC	N-acetyl cysteine
Na_v	Voltage-gated sodium channel
PCr	Phosphocreatine
P_i	Inorganic Phosphate
ROS	Reactive oxygen species
RYR	Ryanodine receptor
SR	Sarcoplasmic reticulum
SRF	Serum response factor
T_m	Tropomyosin
T_n	Troponin

ACKNOWLEDGEMENTS

First and foremost, I would like to thank my supervisor, Dr. Jean-Marc Renaud, for his guidance, support, unlimited patience, and daily Habs banter. His passion for science and the pursuit of knowledge is infectious and the ultimate motivator. He has pushed me to push myself, and has shown me that I possess skills that I might have never otherwise realized. Thank you, Dr. Krantis and Dr. Bergeron, for your insightful advice and for your continued interest. Brooke, Sheema, Kyle, and Louise, thank you for your friendship, for your support, and making every time in the lab a great one.

Thank you, Mom and Dad, for always being there for me and encouraging me to go on, even when the light at the end of the tunnel seemed dim. You have instilled a great set of values in me, including an appreciation for the value of education. Thank you, Matthew, Rachelle, and Daniel, for always being there for me.

Kathryn, I could never thank you enough for your support and understanding. It means the world to me that you have stood by me throughout and I appreciate the sacrifices you have made. My best memories in Ottawa were the times you would come down to visit. Simon, you made my transition to Ottawa life a smooth one, and made it feel like home. I will never forget your and Jeanette's continual support and hospitality. Thank you for always helping me to keep things in perspective.

TABLE OF CONTENTS

TABLE OF FIGURES

LIST OF TABLES

CHAPTER 1

INTRODUCTION

Muscle contractions are what make movement possible in animals. During a contraction, chemical energy is converted into mechanical energy, the result being force or work. A muscle consists of elongated cellular units know as muscle fibres, each muscle fibre containing many myofibrils, and each myofibril containing sarcomeres, which are the contractile unit. As more muscle fibres in a given muscle are recruited and contract simultaneously, the total force produced by a muscle increases. The energy that powers muscular activity is in the form of adenosine triphosphate (ATP). Though ATP is finite in myocytes, muscular activity is highly demanding in terms of energy. During exercise, utilization of ATP can increase anywhere from 20- to 100- fold, depending on fibre type and activity intensity (Gibbs, 1987). While muscle fibres have mechanisms to increase ATP production in response to increased demand, these mechanisms are not always adequate and cannot be sustained indefinitely. If the gap between ATP demand and supply becomes significant, deleterious ATP depletion can occur and this can lead to impaired muscle function and even fibre damage. There are, however, mechanisms in place to prevent this type of critical ATP depletion.

One such mechanism involves the ATP-sensitive potassium channel (K_{ATP} channel) (Noma, 1983). The K_{ATP} channel remains closed when ATP is present and bound, and opens when ATP is absent (Noma, 1983). Under normal conditions, at rest, intracellular ATP concentration ($[ATP]_i$) levels are elevated and the channel is closed. During periods of heavy ATP utilization that can lead to conditions of high metabolic stress, a drop in $[ATP]_i$ leads to the channel opening, resulting in increased potassium ion (K^+) conductance (G_K). In this

way, the K_{ATP} channel links membrane K^+ permeability to the energy state of the cell, and can be said to act as an energy sensor in myocytes. K_{ATP} channels are activated during metabolic stress to limit ATP depletion (Noma, 1983). More importantly, fibre damage occurs in K_{ATP} channel deficient skeletal muscle following periods of activity, such as running and swimming (Thabet *et al.*, 2005;Kane *et al.*, 2006).

The efflux of K^+ ions that occurs through open K_{ATP} channels as a result of low $[ATP]_i$ levels is an outward current that counteracts the inward current of sodium ions (Na^+) during action potential, reducing action potential amplitude (Gong *et al.*, 2003). This leads to a reduced Ca^{2+} release from the sarcoplasmic reticulum (SR) (Burton & Smith, 1997). This means a reduced activation of the contractile machinery and myosin ATPase activity, as well as a reduced load for Ca^{2+} ATPases that pump Ca^{2+} back into the SR after a muscle contraction. This results in a reduction in ATP utilization and preservation of $[ATP]_i$.

Abolishing K_{ATP} channel activity results in abnormal membrane depolarization exceeding 50 mV in some cases (as opposed to 10-20 mV depolarization under normal conditions) (Gramolini & Renaud, 1997;Cifelli *et al.*, 2007). The lack of K_{ATP} channel activity also leads to abnormal increases in $[Ca^{2+}]_i$ and unstimulated force (Cifelli *et al.*, 2007). Verapamil, a L-type Ca^{2+} channel blocker, prevents the increase in unstimulated force in K_{ATP} channel deficient muscles and it was suggested that the increase in $[Ca^{2+}]_i$ was due to activation of L-type Ca^{2+} channels (Cifelli *et al.*, 2008). Recently the addition of N-acetyl cysteine (NAC), a known scavenger for reactive oxygen species (ROS), to K_{ATP} deficient muscle during fatigue, also results in the effect of reducing the increase in unstimulated force (Boudreault *et al.*, 2010). This opens the possibility that the L-type Ca^{2+} channel is not the only factor leading to the elevated resting tension observed during fatigue in K_{ATP} deficient

muscle. However, it remains to be documented how verapamil and NAC affect myoplasmic $[Ca^{2+}]_i$ during fatigue in K_{ATP} deficient muscle. The objective of this thesis was to test the hypothesis that "the increase in resting $[Ca^{2+}]_i$ during fatigue in K_{ATP} channel deficient muscles starts with an excess Ca^{2+} influx through L-type Ca^{2+} channels, followed by an excess ROS production that causes a further increase in resting $[Ca^{2+}]_i$".

Muscle contraction

Muscles generate force through an excitation-contraction coupling mechanism. At rest, membrane potential (E_m) in a myocyte is about -75 mV (Matar *et al.*, 2000;Lannergren & Westerblad, 1987). This resting E_m is largely maintained by ClC-1 chloride channel, K_{ATP} channel, and the Kir2.1 inward rectifier channel (Pedersen *et al.*, 2009;Lindinger & Heigenhauser, 1991;Liu *et al.*, 2001). Signal generation in the central nervous system (CNS) propagates in the form of an action potential (AP) through the axon of the α-motorneuron (Merton, 1954). Next, the AP reaches the neuromuscular junction (Westerblad & Allen, 1991), a specialized synapse between the α-motorneuron terminals and synaptic endplates of the muscle fibre cell membrane, the latter being rich in ligand sensitive acetylcholine (ACh) receptors. At this site, ACh is released from the α-motorneuron and binds the ACh receptors in the muscle fibre membrane, causing a conformational change and the opening of the receptor pore.

Upon opening of the pore, Na^+ and K^+ pass through the cell membrane. Na^+ driving force through the Ach receptors is greater than that of K^+, so the net effect is a localized depolarization. This localized depolarization activates voltage-sensitive Na^+ (Na_V) channels, leading to a more intense and rapid influx of Na^+. E_m reaches about 30 mV at the peak of the

AP (Matar *et al.*, 2000;Lannergren & Westerblad, 1987). This is also when Na_V channels inactivate to cease Na^+ current, while voltage-sensitive K^+ channels are activated to permit K^+ efflux. This K^+ efflux has the opposite effect of the Na^+ influx leading to the repolarization of the cell membrane back to the resting level. From the neuromuscular junction, the AP propagates along the cell membrane and into the transverse tubules (t-tubules), which are invaginations of the cell membrane that run along and are closely associated with the sarcoplasmic reticulum (SR). Voltage sensitive Ca^{2+} channels $Ca_{V1.1}$, also known as L-type Ca^{2+} channels or dihydropyradine receptors (DHPR), are activated during the AP undergoing a conformational change. In skeletal muscle, these L-type Ca^{2+} channels allow for a small Ca^{2+} influx, and more importantly, they interact physically with the SR Ca^{2+} release channels, called ryanodine receptors (RYR). Activation of RYR triggers a much larger Ca^{2+} release from the SR into the cytosol.

The sarcomere is the contractile unit that produces force in skeletal muscle. It is comprised of thick filaments containing myosin, one of the contractile proteins, and thin filaments containing actin, the other contractile protein, as well as troponin (T_n), and tropomyosin (T_m), two regulatory proteins. Each tropomyosin molecule is associated with one troponin molecule, the latter composed of three subunits: C, I and T. In the thin filament, tropomyosin blocks the myosin binding site on actin, 1 T_m covering 7 actins. As $[Ca^{2+}]_i$ increases, it binds to troponin C. The Ca^{2+}-T_n complex then shifts the tropomyosin away from the myosin binding site. As myosin binds actin forming a cross-bridge, it undergoes a power-stroke pulling the thin filament towards the sarcomere's centre, releasing ADP and Pi. Binding of ATP to myosin allows the latter to detach from actin. Soon

thereafter, Ca^{2+} is actively transported back into the SR via Ca^{2+} ATPases. When $[Ca^{2+}]_i$ decreases and troponin is liberated of Ca^{2+}, the muscle relaxes.

Fatigue

Fatigue can be defined as a transient recoverable decline in muscle force and/or power with repeated or continuous muscle contractions (McKenna *et al.*, 2008). As producing force is a main function of muscle, a reduced capacity to produce force is often used to measure the stage of fatigue (Westerblad *et al.*, 1998). Fatigue can be caused anywhere from signal generation (central nervous system) to the final site of force production (sarcomere). In one study looking at fatigue, human subjects were asked to voluntarily contract the abductor pollicis muscle until fatigue was observed (Merton, 1954). There was no improvement in force production with direct stimulation to the ulnar nerve, suggesting that fatigue occurred independently of the central nervous system and that the cause of fatigue was within skeletal muscle fibres themselves (Merton, 1954;Vollestad *et al.*, 1988). While a potential role for central fatigue remains a controversy (MacIntosh & Fletcher, 2012), there is now ample evidence to suggest that the primary mechanisms of fatigue are intrinsic properties of skeletal muscles.

Energy balance: 'raison d'être' of muscle fatigue

Proper functioning of muscle requires energy to be readily available in the form of ATP. The largest contributors to the consumption of ATP during muscle activity are (1) the Na^+/K^+ pump responsible for maintaining the Na^+ and K^+ concentration gradients necessary for action potential generation (Clausen, 1996); (2) the myosin-ATPase, which converts chemical energy into mechanical energy; and (3) the Ca^{2+} ATPase responsible for pumping

Ca^{2+} ions back into the SR following a contraction (Gibbs, 1987). During periods of contractions, a fibre's metabolic needs can increase to 100-fold above that of resting levels (Gibbs, 1987). In any cell, ATP is finite and an increase in muscle activity means that ATP production needs to increase as well.

ATP is produced in 5 different ways: (1) hydrolysis of phosphocreatine (PCr) to transfer the high energy phosphate (P_i) to adenosine diphosphate (ADP) (Tortora & Reynolds-Grabowski, 2003):

$$PCr + ADP \leftrightarrow Cr + ATP$$

(2) glycolysis in which glucose (from extracellular spare and intracellular glycogen) is converted to pyruvate (Champe *et al.*, 2005); (3) oxidative phosphorylation, which requires oxygen, uses pyruvate through the Krebs cycle (Champe *et al.*, 2005); (4) fatty acid β-oxidation producing acetyl CoA which then enters the Krebs cycle; and (5) the ADP myokinase reaction:

$$2ADP \leftrightarrow ATP + AMP$$

The production of ATP is kept favoured in this reaction by the deamination of AMP to IMP. The amount of ATP generated when pyruvate is converted to lactate is only 2 ATP molecules per glucose whereas the full oxidation of glucose by the Krebs cycle and oxidative phosphorylation leads to production of 6 ATP through glycolysis and 30 ATP through Krebs cycle for a total of 36 ATP molecules. Fatty acid β-oxidation leads to the production of 14 ATP molecules per oxidation cycle.

As long as ATP production and utilization are kept in balance, muscular function continues unhindered. The metabolic pathways used for ATP production depends on exercise intensity, exercise duration and muscle fibre type being utilized. During sprint-like

exercises, during which a short intense effort is put forth, glycolytic fast-twitch IIB and IIX fibres are recruited and these fibres use glycolysis as the primary sources of ATP with large production of lactic acid. Because of the low ATP production, such fibres will rapidly lose ATP leading to metabolic stress. Low intensity, long duration exercises such as marathon-type exercises, during which a sustained sub-maximal effort is put forth, oxidative slow-twitch fibre types I and IIA fibres are recruited, and oxidative phosphorylation the primary ATP provider. Being more efficient in generating ATP, such exercise can last a long time. However, there is a point when glycogen stores are depleted to a critical level, and when it is reached the capacity of a muscle fibre to generate force diminishes (Chin & Allen, 1997). Thus, whatever type of exercise, eventually the demand for ATP exceeds the capacity for ATP production and $[ATP]_i$ decreases. This results in a metabolic stress, and if ATP depletion is prolonged or severe, the result can be fibre damage and even cell death. Thus, a protective mechanism is required to reduce severe ATP depletion. This protective mechanism involves fatigue, which is now considered a protective mechanism that prevents large depletion of energy reserve and excessive increase in $[Ca^{2+}]_i$, two situations that can lead to fibre damage and death (McKenna *et al.*, 2008).

Role of metabolites in the decrease in force during fatigue at the sarcomere level

A major consequence of all the metabolic pathways producing ATP is the generation of end-products that can affect the force generated at the sarcomere level. Together, the creatine kinase reaction and adenylate kinase reaction combined with the ATP hydrolysis by various ATPases leads to increases in ADP, AMP, IMP, and P_i and decreases in ATP (Allen & Orchard, 1987). Also, lactate and H^+ are produced in large amounts in glycolytic fibres (Cady *et al.*, 1989).

Using skinned fibre preparation, several studies have determined how these metabolites affect force generation at the level of the sarcomere (Fryer *et al.*, 1995). In most studies, ATP levels go down by less than 20% and this level of change has no effect on force generation (Jacobs *et al.*, 1982;Bangsbo *et al.*, 1990). Even larger decreases in ATP up to 80% (Karatzaferi *et al.*, 2001) would not contribute to the decrease in force during fatigue because when ATP is less than 1 mM, force increases. Similarly, an increase in ADP results in an increase in force, not a decrease. AMP, IMP, and lactate have no effect on force generation at the sarcomere level (Jacobs *et al.*, 1982;Bangsbo *et al.*, 1990;Karatzaferi *et al.*, 2001). While a decrease in pH to 6.8-6.4 reduces force at low temperature, it does not at temperatures close to the physiological temperature of 37°C (Westerblad & Allen, 1993b). Of all the changes in metabolites, only the increase in P_i to 30 mM may be important.

P_i accumulation leads to force depression by decreasing the Ca^{2+} sensitivity of the sarcomere (Blanchard & Solaro, 1984) so that at a given submaximal $[Ca^{2+}]_i$, force generation is less at elevated P_i (Debold *et al.*, 2006). At supra-maximal $[Ca^{2+}]_i$ that fully activates the sarcomere, 30 mM P_i decreases force by ≈ 20%, which is much lower than the 80% decrease in force during fatigue (Debold *et al.*, 2006). Consequently, the mechanism of muscle fatigue is upstream of the force generation at the level of the sarcomere.

Fatigue involves a decrease of Ca^{2+} release by SR

During repetitive tetanic contraction leading to fatigue, tetanic $[Ca^{2+}]_i$ first increases by 10-40% during a time when force decreases by about 10% (Fig. 1.1A,B). It has been suggested that the decrease during the first phase (P1) is due to the increase in P_i. P1 is then followed by a stable period (P2) with no change in force output. As the time interval between contractions decreases during the third period (P3), force decreases drastically and

Figure 1.1

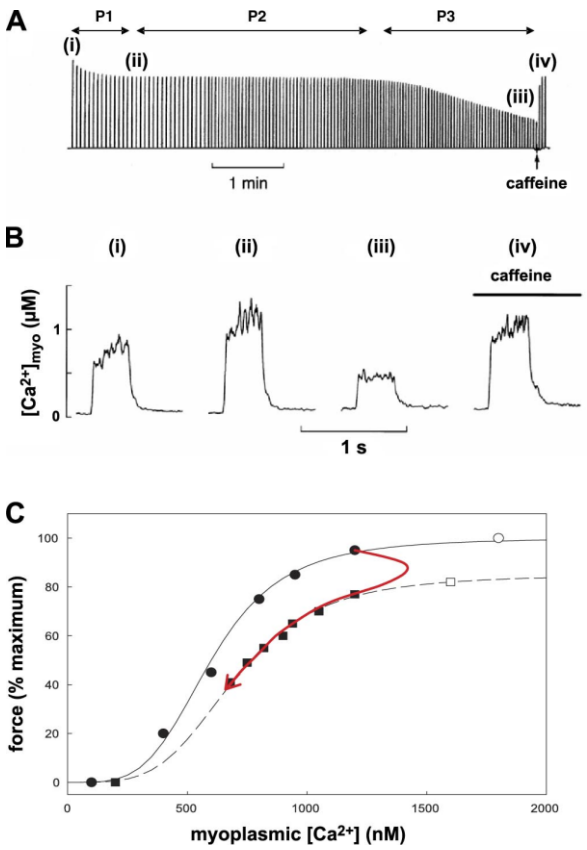

Figure 1.1. Contribution of impaired Ca^{2+} release to muscle fatigue (Westerblad & Allen, 1993a). A) Force recording of repeated tetani continued until force declined by 40%. 350 ms tetani stimulated at 70 or 100 Hz were initially repeated every 4 sec and the tetanic interval was gradually reduced every second minute until force had fallen to about 30% of the original. Force decline was characterized by 3 phases: in P1 force shows a small decline; during P2 force is stable; in P3 the rate of decline accelerates. B) $[Ca^{2+}]_i$ traces for tetani representative of the 3 phases in A, and with the application of 10 mM caffeine. C: steady-state $[Ca^{2+}]_i$-tension relationship. (•) represents unfatigued muscle. (○) represents application of caffeine in unfatigued muscle. □ represents muscle in P3 of fatigue. (□) represents final application of caffeine after fatigue.

this is associated with a decrease in $[Ca^{2+}]_i$ during contractions. Adding caffeine, a RYR opener, restores $[Ca^{2+}]_i$ and force to almost pre-fatigue levels. This suggests that there is sufficient Ca^{2+} in the SR for full force production, even after fatigue. Furthermore, force is almost fully restored, and this is further evidence that the capacity of the sarcomere to produce force is basically unaltered during fatigue as long as $[Ca^{2+}]_i$ is supra-maximal. Then one must ask whether the decrease in $[Ca^{2+}]_i$ is large enough to be the cause of the force decrease. According to the pre-fatigue force-Ca^{2+} relationship (Fig. 1.1C), the $[Ca^{2+}]_i$ during a tetanus in unfatigued fibres, here named tetanic $[Ca^{2+}]_i$, is high enough to cause maximum force development. However, the level of tetanic $[Ca^{2+}]_i$ at the end of the fatigue period is less than 0.5 μM, a level insufficient to fully activate the sarcomere, resulting in a larger decrease in force. The decrease in force at submaximal $[Ca^{2+}]_i$ is then greater as the force-$[Ca^{2+}]_i$ relationship of fatigued fibres is shifted towards greater $[Ca^{2+}]_i$, possibly due to an effect of P_i. This study and others (Allen *et al.*, 2008) have now clearly established that fatigue is primarily associated with a decrease in Ca^{2+} release by the SR resulting in submaximal activation of the sarcomere, and less force production.

The next question is what is (are) the cause(s) of the decrease in Ca^{2+} release from the SR. The possibilities include: (1) a reduction in membrane excitability (i.e. the capacity to generate AP); (2) a decreased response of DHPR to the AP depolarization; (3) a decreased response of RYR to DHPRs; and (4) P_i entering the SR and buffering Ca^{2+}, reducing free Ca^{2+} available for release (Fryer *et al.*, 1995).

There is currently no published study on the potential role of DHPR and RYR in the etiology of muscle fatigue. Conversely, there is a large body of evidence suggesting a decrease in membrane excitability during fatigue. Considering that the objective of this

study is about K_{ATP} channel effects during fatigue, the remainder of the introduction will focus briefly on membrane excitability, and then on the K_{ATP} channel.

Membrane excitability and fatigue

An action potential results in a Na^+ influx and an efflux of K^+. While the Na^+/K^+ ATPase is responsible for pumping Na^+ out of and K^+ into the fibres, change in $[Na^+]_i$ and $[K^+]_i$ occur during muscle activity.

Extracellular $[Na^+]$ ($[Na^+]_e$) does not change significantly due to water influx into muscle fibres (Lindinger & Heigenhauser, 1991). At rest, $[Na^+]_i$ is 8-14 mM, and can increase to 10-58 mM with fatigue (Cairns *et al.*, 2003). This increase in $[Na^+]_i$ results in a 2- to 4-fold decrease in the Na^+ concentration gradient (Nagaoka *et al.*, 1994;Fong *et al.*, 1986). As the Na^+ gradient is reduced, action potential amplitude and excitability are also reduced (Cairns *et al.*, 2003). A two-fold reduction in the Na^+ gradient has no effect on force, while a 3-fold reduction has a small effect on force. Most of the time, under physiological conditions, this point is seldom reached (Cairns *et al.*, 2003). Thus, by itself, Na^+ contributes little to the decrease in membrane excitability, and thus force, during fatigue.

During exercise, $[K^+]_e$ increases from 4.5 to 10 mM in conjunction with decreases in $[K^+]_i$ (Cairns *et al.*, 1995). The direct effect of a reduction in $[K^+]$ gradient is a depolarization of resting E_m from -80 mV to -70 (Lannergren & Westerblad, 1986). As a consequence of the depolarization, there is an increase in Na_v inactivation and a reduction in AP amplitude (Adrian *et al.*, 1970). A large increase in $[K^+]_e$ reduces membrane excitability (Bouclin *et al.*, 1995;Nielsen *et al.*, 1998), but the increase in $[K^+]_e$ appears to cause much smaller decrease in force than what is observed during fatigue. While the Na^+ and K^+ effects

by themselves are not significant, concomitant small decreases in Na^+ and K^+ gradient synergistically depress membrane excitability and force in a way that can account for half of the decrease observed during fatigue (Bouclin *et al.*, 1995).

More recent studies have now demonstrated that the K^+ effects may also depend on the activity of the Cl^- channel (CLC-1) (Pedersen *et al.*, 2005). About 15% of the CLC-1 channels are active at rest. At the onset of exercise, Cl^- conductance decreases by 60-70% as CLC-1 channels close. This prevents the K^+-induced force depression (Pedersen *et al.*, 2003;Ronner *et al.*, 1991). This occurs because during an AP there is an inward Cl^- current that works against the Na^+ influx. At normal $[K^+]_e$ the Cl^- current barely affects the AP depolarization phase, but due to a decreased Na^+ conductance it has a greater inhibitory effect at elevated $[K^+]_e$ (Pedersen *et al.*, 2005). When G_{Cl} decreases, there is less opposition to the positive Na^+ influx allowing for greater depolarization during AP at elevated $[K^+]_e$. Interestingly, when a metabolic stress develops, not only is the K_{ATP} channel activated, but so are the CLC-1 channels up to three times above resting levels (Pedersen *et al.*, 2009). This then has the reverse effect of the decrease in Cl^- conductance. It now allows more Cl^- influx further reducing the extent of the depolarizing Na^+. By lowering AP amplitude, it decreases Ca^{2+} release and force production; i.e. it causes fatigue. The other ion channel that has a large effect on excitability in muscle that has undergone repetitive stimulation is the K_{ATP} channel.

K_{ATP} channel

The K_{ATP} channel is a ligand-gated ion channel that links cell metabolism to excitability in many cell types in the body, including pancreatic β cells, brain, heart, skeletal

and smooth muscle cells (Noma, 1983;Misler *et al.*, 1986;Ashcroft & Kakei, 1989). It regulates cellular function and activity by causing changes in K^+ conductance (G_K), in reaction to variations in $[ATP]_i$.

K_{ATP} channel molecular structure

The K_{ATP} channel is an octomer of four Kir6 subunits that make up the channel pore. Each Kir6 subunit is associated with one regulatory sulfonylurea receptor (SUR) subunit (Clement IV *et al.*, 1997;Inagaki *et al.*, 1997;Shyng & Nichols, 1997). Three-dimensional reconstruction of a K_{ATP} channel complex suggests a central Kir6.2 tetramer closely surrounded by four SUR1 subunits (Mikhailov *et al.*, 2005) (Fig. 1.2).

The Kir6 subunits are members of the inward K^+ rectifier superfamily (Seino, 1999). So far, three Kir6.x genes have been cloned and sequenced: Kir6.1, Kir6.2 and Kir6.3 (Fig. 1.2) (Seino, 1999). Each Kir6 subunits is characterised by two transmembrane domain segments: M1 and M2, forming the pore of the channel (Reimann & Ashcroft, 1999). The H5 loop is located between M1 and M2 and forms the selectivity filter for K^+ (Seino, 1999). The N-terminal of a Kir channel consists of a helix that lies parallel to the membrane surface, and then extends outwards. The C terminus generates a series of β-sheets that form a cytoplasmic corridor that acts as an extension to the permeation pathway into the cytoplasm (Kuo *et al.*, 2003;Tao *et al.*, 2009) (Fig 1.2). The SUR subunit is a member of the ATP-binding cassette (ABC) transporter protein family, of which there are 49 members in the human genome including ABCG1 involved in cholesterol transport, and ABCC7, also known as CFTR (cystic fibrosis transmembrane conductance regulator), which is a chloride channel implicated in cystic fibrosis (Vasiliou *et al.*, 2009). To date, two SUR genes have been

Figure 1.2

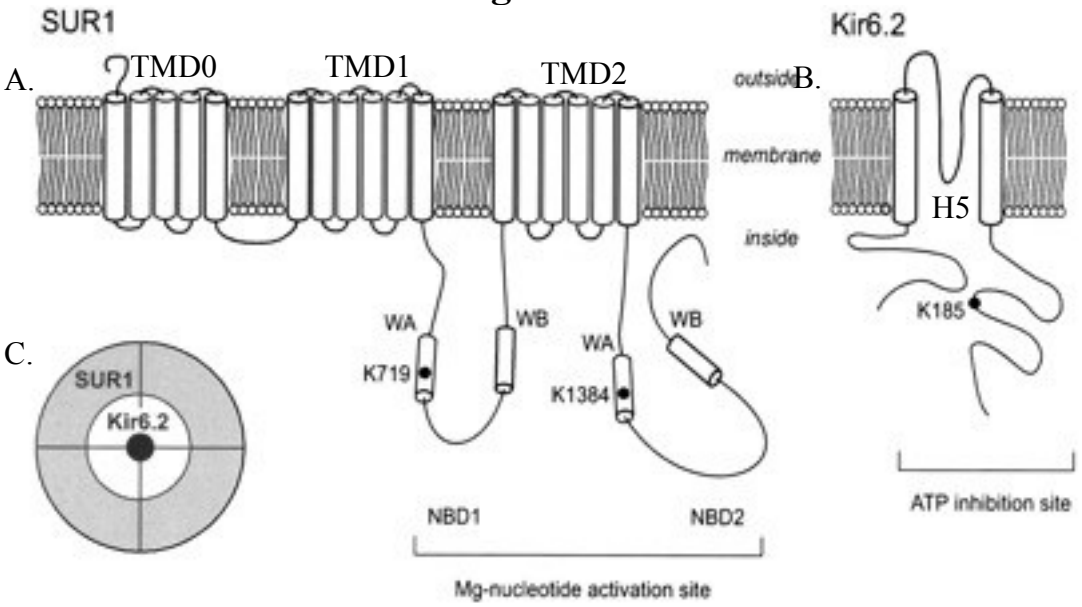

Figure 1.2. Topology of SUR1 and Kir6.2. A) SUR1 is characterized by 17 transmembrane regions which can be grouped into three major transmembrane domains (TMD0, TMD1, and TMD2). Two nucleotide-binding domains (NBD1 and NBD2) are involved in regulation. B) Kir6.2 is characterized by two transmembrane domains (M1 and M2), connected by the pore-forming H5 loop. C) K_{ATP} channel complex suggests a central Kir6.2 tetramer closely surrounded by four SUR1 subunits.

identified: SUR1 and SUR2 (Seino, 1999). This superfamily is characterized by several transmembrane segments and nucleotide binding folds (NBF) (Dean *et al.*, 2001). SUR1 has 17 transmembrane regions, which can be grouped into three major transmembrane domains (1-5 is TMD0, 6-11 is TMD1, and 12-17 is TMD2). TMD0 and TMD1 are connected by a long cytosolic loop containing the nucleotide-binding domain-1 (NBD1). A second nucleotide binding domain (NBD2) is located at the C terminus of TMD2 (Babenko *et al.*, 1998;Nichols, 2006;Hibino *et al.*, 2010) (Fig. 1.2A).

Regulation of K_{ATP} channel activity

K_{ATP} channel opening is inhibited upon ATP binding to the intracellular portion of the Kir6 subunit (Drain *et al.*, 1998;Shyng *et al.*, 1997). K^+ influx through the channel is reduced to 50% of full capacity (K_i) at $[ATP]_i$ of 172 μM (Tanabe *et al.*, 1999). In the absence of Mg^{2+}, ADP also blocks channel activity (Kakei *et al.*, 1985;Noma, 1983) but with lower affinity than ATP, with a K_i of 500 μM. Each Kir subunit forming the tetrameric pore can bind one ATP molecule (Antcliff *et al.*, 2005). In the presence of Mg^{2+}, both ATP and ADP stimulate channel activity through interaction with the SUR subunit (Dunne & Petersen, 1986;Gribble & Ashcroft, 1999); i.e. the regulation of the channel activity by ATP and ADP is a complex one. The nucleotide-binding domains of the SUR subunits contain the binding sites for Mg^{2+}-ATP, and Mg^{2+}-ADP, stimulating K_{ATP} function (Campbell *et al.*, 2004). Physical interaction between the cytoplasmic NH_2 terminus of Kir6.2 and the TMD0 domain of SUR has been shown to be important in regulating Kir6.2 gating by SUR (Babenko & Bryan, 2003).

In pancreatic β-cells the K_{ATP} channel activity is largely dependent on the ATP/ADP ratio as the SUR1/Kir6.2 complex is expressed (Aguilar-Bryan & Bryan, 1999). However, in

cardiac and skeletal muscle where the SUR2/Kir6.2 is expressed, changes in ATP/ADP ratio is not large enough to activate the K_{ATP} channel. There is evidence, however, that K_{ATP} channel becomes active during fatigue, hypoxia, anoxia, and metabolic inhibitions in both cardiac and skeletal muscle due to other metabolites that affect K_{ATP} channel activity, mainly pH, lactate, and adenosine.

It has been shown that K_{ATP} channel activity increases when the decrease in pH_i that occurs during fatigue is mimicked in unfatigued muscle (Standen *et al.*, 1992;Davies *et al.*, 1992). Protons act to decrease the channel sensitivity to inhibitory ATP (Cui *et al.*, 2006) as ATP half-inhibition of the channel activity increases from 17 μM at pH 7.2 to 260 μM at pH 6.3 under patch clamp condition (Davies, 1990). Lactate also activates the channel under normal ATP concentrations, at least in cardiac muscle, and this effect can be abolished by blocking K_{ATP} channels with the drug glibenclamide (Keung & Li, 1991).

Finally, adenosine is a metabolite that is released from metabolically challenged myocytes and stimulates K_{ATP} channel activity in ventricular myocytes (Ito *et al.*, 1994;Kirsch *et al.*, 1990) and skeletal muscle (Barrett-Jolley *et al.*, 1996). This is achieved through a G protein signalling cascade. PKC-dependent cardiac preconditioning by adenosine indicates an important role for adenosine in K_{ATP} channel mediation in vivo, however it remains unclear whether sarcolemmal or mitochondrial K_{ATP} channels are both immediate targets (Cohen *et al.*, 2008). So, changes in metabolites associated with fatigue are large enough to activate the K_{ATP} channel. More importantly, there is evidence that metabolic stress such as fatigue or ischemia results in K_{ATP} channel activation.

Physiological roles of K_{ATP} channel

The K_{ATP} channel has three major physiological roles: (1) it is involved in glucose homeostasis; (2) it plays a role in blood flow regulation; (3) and it plays a myoprotective role in cardiac and skeletal muscle. In regard to glucose homeostasis, it is involved in the secretion of insulin and the inhibition of glucagon secretion under hyperglycemic conditions (Craig *et al.*, 2008). The K_{ATP} channel is also involved in glucose sensory neurons at the level of the hypothalamus, and these neurons regulate feeding behaviour and glucagon secretion (Miki *et al.*, 2001). K_{ATP} channel activity has been shown to affect blood flow. Knocking out Kir6.1 gene in mice results in high blood pressure. These mice have a harder time exercising than wild type mice, and intense exercise can even result in death in these animals. K_{ATP} channel is also involved in increasing blood flow in skeletal muscle during muscular activity (Standen et al., 1989). Most importantly for the objective of this thesis, is the myoprotective effect of K_{ATP} channel.

Myoprotection

There is a large body of evidence to suggest a myoprotective role of K_{ATP} channels in cardiac and skeletal muscle. For both cardiac and skeletal muscles, in the absence of metabolic stress, there are no functional differences between muscles from wild-type mouse and those from Kir6.2$^{-/-}$ mouse, which do not express functional K_{ATP} channel (Nichols, 2006;Thabet *et al.*, 2005). The same is not true during a metabolic stress (Zingman *et al.*, 2002). When Kir6.2$^{-/-}$ mice are made to run on a treadmill, the result is often death (73% mortality) due to cardiac arrhythmia associated with the lack of K_{ATP} channel activity (Zingman *et al.*, 2002). Kir6.2$^{-/-}$ mice also demonstrated a faster rate of fatigue during a

single bout of running, averaging only a distance of 0.9 km of running at 20 m/min, compared to 2.2 km for wildtype mice at the same speed and 0° incline (Thabet *et al.*, 2005). Following a four-week period of daily running at 24 m/min and 20° incline, 25% of EDL fibres and 12% of plantaris and tibialis fibres from Kir6.2$^{-/-}$ mouse showed signs of fibre damage and regeneration (Thabet *et al.*, 2005). Ninety-nine percent of fibres showing signs of damage were type IIB fibres. The same effect was observed in mice lacking SUR2 subunit by means of genetic knockout (Stoller *et al.*, 2009), which also lack functioning K_{ATP} channels. From these studies, it is clear that exercise in K_{ATP} deficient animals results in reduced performance, fibre damage, and even death if animals are exercised vigorously. The mechanisms for the myoprotection against early onset of fatigue and fibre damage involve a control of ATP consumption and Ca^{2+} levels for both cardiac and skeletal muscles.

A main role of K_{ATP} channels in skeletal muscle is their contribution to the onset of fatigue. The application of sulfonylureas has little or no effect on cardiac action potential (Faivre & Findlay, 1989) and contractile function is unaffected in ventricular myocytes from animals without functional K_{ATP} channels due to a genetic knockout (Kir6.2$^{-/-}$). K_{ATP} channels are in a closed state at rest in skeletal muscles in vitro (Light & French, 1994). In cardiomyocytes, when cellular metabolism is hindered by mimicking ischemia, the action potential duration is reduced and there is a reduction in Ca^{2+} release and force production as a result of K_{ATP} channel activation (Cole *et al.*, 1991).

In skeletal muscles, the direct effect of K_{ATP} channel opening is a reduction of action potential amplitude (Gong *et al.*, 2003). This reduction involves two different processes: (1) an increase in K^+ conductance allowing for an outward K^+ current opposing the inward Na^+ current during depolarization (Gong *et al.*, 2003;Matar *et al.*, 2000), and (2) an increase in K^+

efflux during the AP leading to increased $[K^+]_e$, leading to a membrane depolarization and Na^+ channel inactivation, further reducing AP amplitude (Balog *et al.*, 1994;Lannergren & Westerblad, 1986;Renaud & Mainwood, 1985).

The result of reduced AP amplitude is a reduced Ca^{2+} release by the SR causing a reduction in force production (Renaud, 2002). The reduced Ca^{2+} release is beneficial for two reasons: (1) less Ca^{2+} needs to be pumped back into the SR via Ca^{2+} ATPase pumps, and (2) less actin-myosin cross-bridges are established, reducing myosin ATPase activity. The main result of these factors is a conservation of ATP.

Another important mechanism is the maintenance of the resting membrane potential by K_{ATP} channels. Severe contractile dysfunctions occur during fatigue in the absence of channel activity. They include large membrane depolarizations, large increases in unstimulated $[Ca^{2+}]_i$, and large force production during fatigue; it also reduces the capacity to recover force following fatigue possibly due to fiber damage occurring during fatigue (Gramolini & Renaud, 1997;Matar *et al.*, 2000;Cifelli *et al.*, 2007). It has been shown using the L-type Ca^{2+} blocker verapamil that excess membrane depolarization in the absence K_{ATP} channels is large enough to increase Ca^{2+} influx through L-type Ca^{2+} channels and can be a direct cause of fibre damage in cardiac muscle (Zingman *et al.*, 2002;Baczko *et al.*, 2005). Although Ca^{2+} influx and the accompanying depolarization is not necessary to activate Ca^{2+} release in skeletal muscle, due to close interaction between L-type Ca^{2+} channel and RYRs, it was still shown that adding verapamil to K_{ATP} deficient FDB muscle results in a reduction of the large unstimulated force seen in these muscles during fatigue, as well as a reduced rate of fatigue (Cifelli *et al.*, 2008). In Cifelli's 2008 study, however, force was measured but $[Ca^{2+}]_i$ was not. From these results, it was suggested that the large increase in unstimulated

force during fatigue in K_{ATP} deficient FDB muscle is due to excess Ca^{2+} influx through L-type Ca^{2+} channels, due to the increased depolarization during fatigue in the absence of normal K_{ATP} channel activity. This excess $[Ca^{2+}]_i$ can lead to fibre damage reference, which leads to an increased rate of fatigue. One objective of this study was thus to document how verapamil affects unstimulated and tetanic $[Ca^{2+}]_i$ during fatigue in K_{ATP} channel deficient muscle.

NAC also abolishes resting tension in $K_{ATP}^{-/-}$ muscle

Excessive rise in $[Ca^{2+}]_i$ can lead to an increased ROS production in the mitochondria (Inoue *et al.*, 2003). ROS affects muscle activity by numerous mechanisms, including increasing the open probability of RYR1 (Anzai *et al.*, 2000), decreasing reuptake by the SR Ca^{2+} ATPase, and increasing leakiness through the SR Ca^{2+} pumps (Lee & Okabe, 1995;Senisterra *et al.*, 1997). ROS, such as hydrogen peroxide, have also been shown to stimulate L-type Ca^{2+} channels (Chaplin & Amberg, 2012). All of these factors lead to an increase in $[Ca^{2+}]_i$. ROS can also reduce Ca^{2+} sensitivity of the contractile proteins, and result in reduced force production in single FDB muscle fibres (Moopanar & Allen, 2005;Gariepy-Boudreault, 2010). The implication here is that ROS is having an effect on contractility either at the level of $[Ca^{2+}]_i$ or Ca^{2+} sensitivity. In fact, it has recently been shown that NAC has a similar reducing effect on unstimulated force during fatigue in K_{ATP} channel deficient muscle (Gariepy-Boudreault, 2010). This suggests the possibility that Ca^{2+} influx through L-type Ca^{2+} channels is not the only factor at play.

In the studies on the verapamil and NAC effects, unstimulated and tetanic force was measured, but not myoplasmic Ca^{2+}. It therefore remains to be determined how $[Ca^{2+}]_i$ between and during contraction is affected by these compounds.

Objective and hypothesis

The **overall objective** of this study was to determine the contribution of the L-type Ca^{2+} channels and ROS to the unstimulated force during fatigue in K_{ATP} channel deficient FDB muscle fibres. The **hypothesis** is that "the increase in resting $[Ca^{2+}]_i$ during fatigue in K_{ATP} channel deficient muscles starts with an excess Ca^{2+} influx through L-type Ca^{2+} channels, followed by an excess ROS production that causes a further increase in resting $[Ca^{2+}]_i$". To test this hypothesis, two aims were pursued. **Aim #1**: to demonstrate that verapamil reduces unstimulated $[Ca^{2+}]_i$ during fatigue in K_{ATP} deficient FDB single fibres, and results in a slower decrease in tetanic $[Ca^{2+}]_i$ during fatigue. **Aim #2**: to demonstrate that NAC will not prevent an initial rise in $[Ca^{2+}]_i$ due to activation of L-type Ca^{2+} channels, but will partially block the elevated $[Ca^{2+}]_i$ that develops later during fatigue.

The experimental approach involved the use of single FDB muscle fibres separated by trituration following a collagenase digestion. While this approach had been successfully used by Cifelli et al. (2007) to measure Ca^{2+}, problems had then arisen afterward in terms of adequate fibre viability and stability. Furthermore, no study to date exists documenting the importance of various factors such as the nature of the culture media during the collagenase digestion and the composition of the physiological solutions during Ca^{2+} measurements. Therefore, a third aim was added to this study. That is, to document how MEM, DMEM and

FBS affect the morphology and contractile characteristics of single FDB fibers as well as the stability of those fibers over long incubation periods.

CHAPTER 2

METHODS AND MATERIALS

Animals and K_{ATP} channel deficient muscle fibres

Experiments were carried out using single fibres from flexor digitorum brevis (FDB) muscles from CD-1 (Charles River, Canada) and Kir6.2$^{-/-}$ mice (provided by Dr. S Seino, University of Kobe, Japan). K_{ATP} channel deficient muscle fibres were obtained by (1) exposing fibres from CD-1 mice to glibenclamide, a K_{ATP} channel inhibitor (pharmacological model) and (2) by using Kir6.2$^{-/-}$ fibres, a genetic model that does not express functional K_{ATP} channels in skeletal muscle (Zhang *et al.*, 2002). Mice were two to four months in age and weighed 20-30 g. Mice were fed *ad libitum*, and housed according to the guidelines of the Canadian Council for Animal Care (CCAC). The Animal Care Committee of the University of Ottawa approved all experimental procedures used in this study. Mice were anaesthetized with a single intraperitoneal injection of 2.2 mg ketamine, 0.44 mg xylazine and 0.22 mg acepromazine per 10 g of body mass. Subjects were then sacrificed by cervical dislocation.

Single fibre preparation

Single fibres were isolated from FDB bundles by a method involving collagenase digestion. FDB muscles were incubated 3 h at 37°C in culture medium containing 0.2% (w/v) collagenase type I (Worthington, USA) with or without 10% heat inactivated foetal bovine serum (FBS, Gibco, Canada), 100 units/ml of penicillin and 100 μg/ml of streptomycin (Gibco, Canada). Two culture media were tested: i) minimum essential

medium with Earle's salt and L-glutamine (MEM, Gibco, Canada) and ii) Dulbecco's Modified Eagle Medium High Glucose (DMEM, Gibco Canada). Following incubation, fibres were separated by gentle trituration in three ml of collagenase-free culture medium. Aliquots (100 μM) of concentrated fibre-containing medium were then placed on Matrigel (VWR, Canada) pre-coated 12 mm diameter coverslips (VWR, Canada). Fibres were incubated another 30 min to allow for fibres to settle on the matrigel and become attached. Culture medium was then added to cover the entire coverslip with fibres attached and incubated for at least another 30 min before being used for Ca^{2+} or sarcomere length measurements.

Experimental setup & solutions

Coverslips containing single FDB fibres were mounted into a 370 μl chamber (model RC-25, Warner Instruments, USA). The preparations were continuously perfused in physiological solution with a flow rate of 5 ml/min. Experimental temperature of either 25°C or 37°C was controlled for by simultaneously heating the plate in which the chamber was mounted, and pre-heating the physiological solution, using a dual channel heater controller (model TC-344B, Warner Instruments, USA).

The control physiological solution contained (mM): 118.5 NaCl, 4.7 KCl, 2.4 $CaCl_2$, 3.1 $MgCl_2$, 25 $NaHCO_3$, 2 NaH_2PO_4 and 5.5 D-glucose. All solutions were continuously bubbled with 95% O_2–5% CO_2 and had a pH of 7.4. Glibenclamide (10 μM)-containing solution was obtained by first dissolving glibenclamide in DMSO and adding it to the physiological solution. Solutions containing N-Acetyl-Cysteine (NAC, 1 mM) or verapamil (1 μM) were obtained by adding NAC or verapamil directly to the saline solution, as these

compounds are water soluble. In all experiments DMSO concentration was kept at 0.1% (v/v).

Fibre stimulation

Fibres were stimulated by field stimulation, generated by two platinum electrodes running along each side of the chamber containing the fibres. The electrodes were connected to a Grass S88 stimulator and SIU5 isolation unit (Grass Technologies, West Warwich, RI, USA) which were used to generate 200 ms trains of 0.4 ms pulses; unless indicated, the stimulation frequency was 120 Hz and voltage 10 V.

$[Ca^{2+}]_i$ measurement

Fibres were loaded with fura-2 by incubating fibres 30 min at 37°C in culture medium containing five μM Fura-2 AM (Molecular Probes, Canada), similar to the protocol described by Westerblad & Allen (1991). Fura-2 AM contains an ester that makes it membrane-permeable. Once in the cytosol, the ester group is cleaved by esterase freeing the Fura-2. The coverslip containing the fibres was then transferred to the experimental chamber. Fura-2 is a ratiometric Ca^{2+} fluorescent indicator. Fura-2 is alternatively excited at wavelengths of 340 and 380 nm, and light emission was measured at 505 nm. As fura-2 binds calcium when free intracellular calcium increases, light emission when excited at 340 nm increases whereas for the excitation at 380 nm it decreases. Light excitation and emission were respectively controlled and measured by an IonOptix dual fluorescent contractility device (USA) containing the following filters: 340 ± 12 nm, 380 ± 6 nm and 505 ± 6 nm. Data acquisition was set at 200 Hz; the fluorescence ratio (R) was calculated by dividing the light emitted for two msec during the excitation of 340 nm (numerator) by the light emitted for two msec

while the excitation was 380 nm (denominator). To be consistent for all fibres, $[Ca^{2+}]_i$ was calculated as previously described using average values for R_{MIN} and R_{MAX} measured in the same fibres (Westerblad & Allen, 1991). Briefly, R_{MIN} was determined by exposing fibres to 10 μM bapta-AM and R_{MAX} using one mM Ca^{2+} and 10 μM ionomycin. The $[Ca^{2+}]_i$ was calculated from the 340/380 fluorescence ratio (R) using the following equation:

$[Ca^{2+}]_i = K_d \bullet \beta \bullet (R - R_{MIN})/(R_{MAX} - R)$ where K_d at 37°C was 224 nM (Li *et al.*, 2010), R_{MIN} 89 ± 0.7% (n = 7 fibres) of the resting ratio, R_{MAX} 126.1 ± 7.5% of the maximum tetanic ratio, and β the fluorescence at 380 nm excitation of Ca^{2+} free divided by Ca^{2+} bound fura-2, being 3.17 ± 0.72. Two parameters are reported in this study. The first parameter is unstimulated $[Ca^{2+}]_i$, which is defined as the $[Ca^{2+}]_i$ when fibres are not stimulated. This term was chosen to be consistent with the term unstimulated force. Unstimulated $[Ca^{2+}]_i$ was determined by averaging the $[Ca^{2+}]_i$ during the 100 ms period preceding a contraction. Tetanic $[Ca^{2+}]_i$ was defined as the maximum $[Ca^{2+}]_i$ observed during a tetanic contraction and determined by averaging the $[Ca^{2+}]_i$ during the tetanic plateau phase.

Sarcomere length measurement

A MyoCam-S High-Speed (up to 250 Hz) Contractility Camera (IonOptix) was used to measure sarcomere length before, and during contractions. Light intensity was analyzed along the length of the muscle fibre, and this allowed for measuring the decrease in the width of I-bands, as fibres contracted. From the change in I-band width, sarcomere length was calculated as described in Fig. 2.1.

Figure 2.1

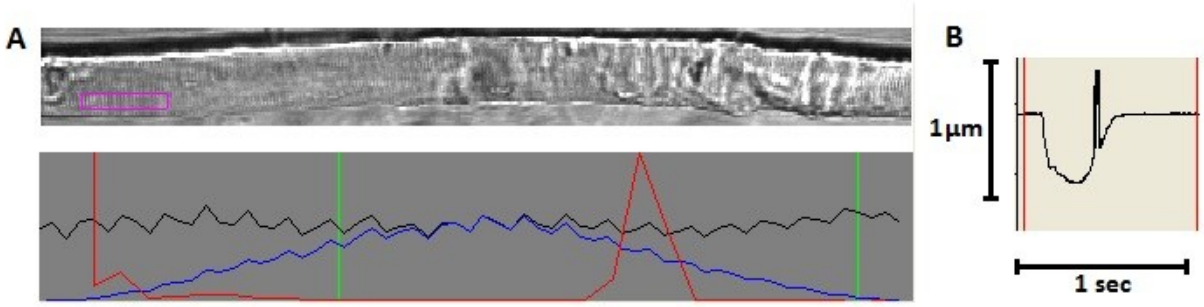

Figure 2.1. Sarcomere length was analyzed using a Fourier analysis of the frequencies of light and dark bands observed longitudinally along the fibre. A) Picture of a fibre with A and I bands seen as alternating light and dark lines (top). The box shows the selection on which the analysis is being performed. The light intensity is mapped and displayed as a black line displaying peaks and dips (bottom). The IonOptix software performs a Fourier analysis and the result is the detection of the most dominant frequency of alternating light and dark (red peak). This frequency is converted to a sarcomere length value using a standard. B) The output generated by the software showing the sarcomere shortening during a tetanic contraction.

Experimental protocol

All fibres were allowed to equilibrate and checked for stability during a 15 min period, during which fibres were stimulated once every 100 s. In experiments employing drug challenge, this period was extended to a 30 min period, the first 15 min being in control solution followed by 15 min in drug-containing solution. This equilibration regimen was followed by a step-wise increase in stimulation frequency covering 10, 30, 40, 50, 60, 70, 80, 100, and 120 Hz, with stimulation once every 100 s. The fibres were then put through a 180 s fatigue protocol, with contractions every second at a frequency of 120 Hz. Finally, the fibres went through a 15-minute recovery period with stimulation every 100 s.

Statistical analysis

ANOVA was used to determine significant differences. Split plot designs were used because fibres were tested at all times and frequency levels. ANOVA calculations were made using the Version 9.0 GLM (General Linear Model) procedures of the Statistical Analysis Software (SAS Institute Inc., Cary, NC USA). When a main effect or an interaction was significant, the least square difference (L.S.D.) was used to locate the significant differences (Steel & Torrie 1980). The word "significant" refers only to a statistical difference ($P<0.05$).

CHAPTER 3

RESULTS

Isolation of viable single fibres

For a study of contractile properties in single fibres using a collagenase digestion to be valid, a proper protocol needed to be developed for the production of viable, contracting single FDB fibres. The use of collagenase to isolate single FDB fibres has been performed in the past, mostly for voltage patch clamp studies and a few contractility studies. For the former, viability of fibres is not a primary concern as only a patch of membrane is utilized to study the properties of ion channels. For contractility studies, however, one must get "viable fibres". For the purposes of this study, viable fibres are fibres that respond to electrical stimuli giving rise to a contraction over as long a period of time as observed with single fibres that are mechanically dissected (Allen *et al.*, 1995). Furthermore, viable fibres are expected to have good morphology and straight appearance (Fig. 3.1A), with clearly discernible A and I bands when observed under the microscope (Fig. 3.1B). The goal was to minimized the occurrence of fibres that appeared damaged and were not straight (Fig. 3.1C) with A and I bands that were not easily discernible (Fig. 3.1D) or fibres that were super-contracted (Fig. 3.1E).

Importance of FBS during the collagenase digestion

Minimum Essential Medium (MEM) and Dulbecco's Modified Eagle Medium (DMEM) are the two most commonly used culture media employed in studies in which

Figure 3.1

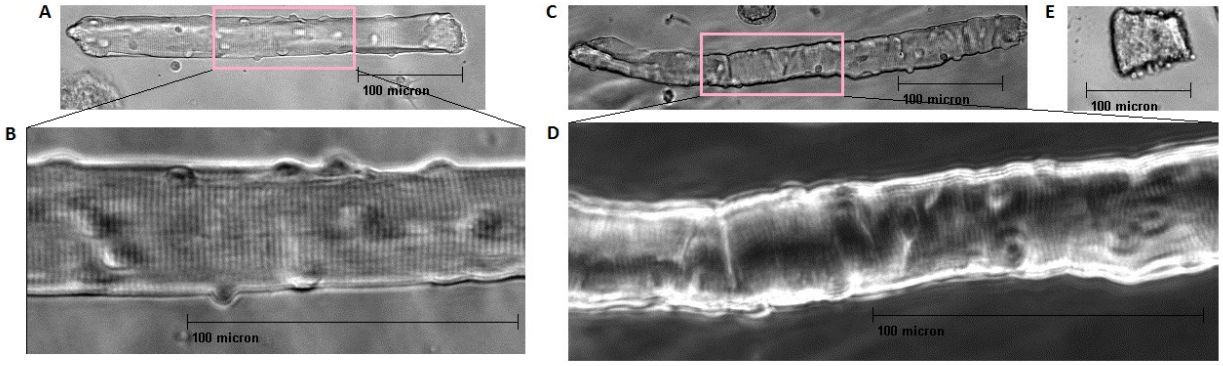

Figure 3.1. Single fibre appearance after a three hour collagenase digestion. A) Example of a straight fibre for which B) clear A and I bands are observed. C) Example of a non-straight fibre with D) membrane folds and non-easily discernible A and I bands. E) Example of a super-contracted fibre.

single muscle fibres are isolated by a collagenase treatment. The major differences between the two being a greater amino acid content in DMEM than in MEM, the presence of glycine, L-serine, and ferric-nitrate only in DMEM, and 25 mM glucose in DMEM compared to 5.6 mM in MEM (Appendix 1). Whether MEM or DMEM was used as the culture medium for collagenase digestion, the medium used was supplemented with 10% (v/v) fetal bovine serum (FBS) as has also been done in previous studies (Cifelli *et al.*, 2007). When 10% FBS was not added in the collagenase-containing MEM or DMEM, all fibres super-contracted before the end of the digestion period (Fig. 3.1E). Thus, 10% FBS was present at all times when MEM or DMEM were used to incubate FDB fibres.

Importance of culture medium and FBS in the physiological solution

Fibre morphology

In physiological solution without FBS under control conditions, a larger proportion (62%) of unstimulated FDB single fibres had a straight morphology when the collagenase digestion had been in MEM as opposed to the digestion in DMEM (23%) (Fig. 3.1A, 3.2A). The addition of 0.2% FBS to the physiological solution had no effect on the number of straight fibres prepared in MEM, but increased the proportion of straight fibres from 23% to 40% for those prepared in DMEM. After fibres were stimulated to fatigue and allowed to recover for 15 minutes, the number of fibres with straight morphology was counted again. For fibres prepared in MEM with no FBS in the physiological solution, a 9% reduction in the number of straight fibres was observed after fatigue. With DMEM as culture medium with no FBS in the physiological solution, there was a slight, but non-significant, increase in the

Figure 3.2

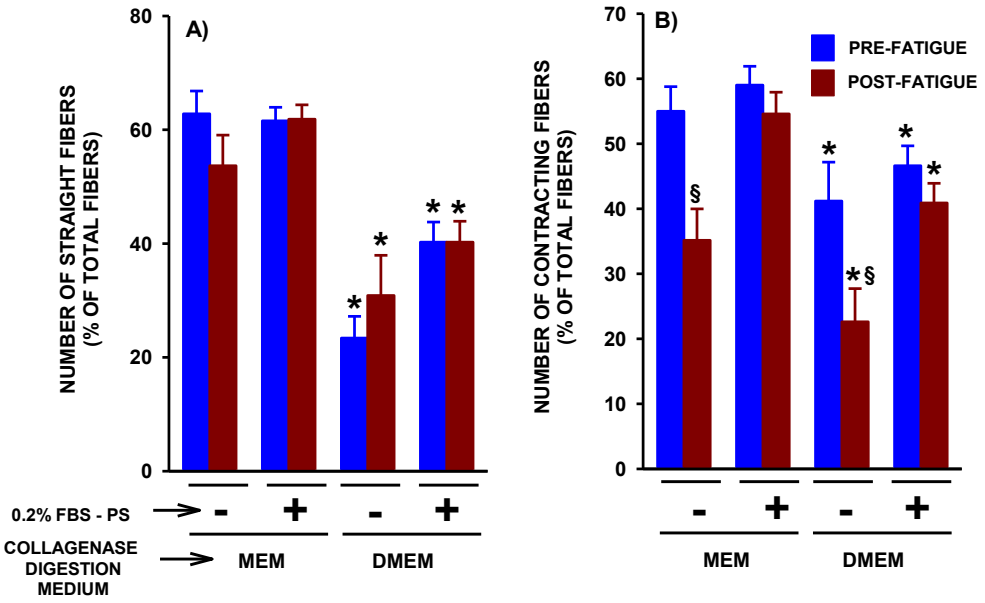

Figure 3.2. Effects of culture medium and FBS on fibre appearance and contractility. Single fibres were separated after a 3-hr digestion in 0.2% (w/v) collagenase in either MEM or DMEM culture media containing 10% (v/v) FBS. During measurements, fibres were superfused with physiological solution in the presence or absence of 0.2% FBS (v/v). Pre-fatigue measurements were performed after a 15 min equilibration period. Fatigue was elicited with one 200 msec long train of 10 V pulses at 120 Hz every sec for three minutes. Post-fatigue measurements were performed after a 10 min recovery period. Numbers of fibres are expressed as a percentage of the total number of fibres on cover slip. Vertical bars represent the S.E. for 109-297 fibres from 6-8 mice.

* Marks a significant difference between MEM and DMEM culture media.

§ Marks a significant difference between pre-fatigue and post-fatigue measurements.

ANOVA L.S.D., $P < 0.05$

number of straight fibres after fatigue. Adding FBS to the physiological solution resulted in no difference in the number of straight fibres before and after fatigue, whether they were incubated in MEM or DMEM.

Fibre contractility

Prior to fatigue and in the absence of FBS in the physiological solution, there were also a greater proportion of contracting fibres, in fibres prepared in MEM, than in DMEM (Fig. 3.2B). 55% of the fibres were contracting after isolation in MEM compared to 41% in DMEM. The addition of 0.2% FBS caused a 5% increase in the number of contracting fibres incubated in MEM or DMEM. After fatigue, the number of contracting fibres for the MEM condition and in the absence of 0.2% FBS in the physiological solution was only 35% compared to 55% prior to fatigue, representing a 20% reduction. A similar situation to that was observed for the DMEM condition as the number of contracting fibres decreased from 41% to 23%. When 0.2% FBS was present in the physiological solution, the reduction in the number of contracting fibres with fatigue was abolished, in fibres prepared in either MEM or DMEM.

Contraction thresholds

The effects of culture medium, presence of 0.2% FBS in the physiological solution, and fatigue were also analyzed with regard to contraction threshold. Figures 3.3-3.5 came from the same data in which the number of contracting fibres, expressed as a percentage of total contracting fibres, is plotted against stimulation strength; each figure emphasizing the effect of either culture medium (Fig. 3.3), 0.2% FBS in the physiological solution (Fig. 3.4), or fatigue (Fig. 3.5).

Figure 3.3

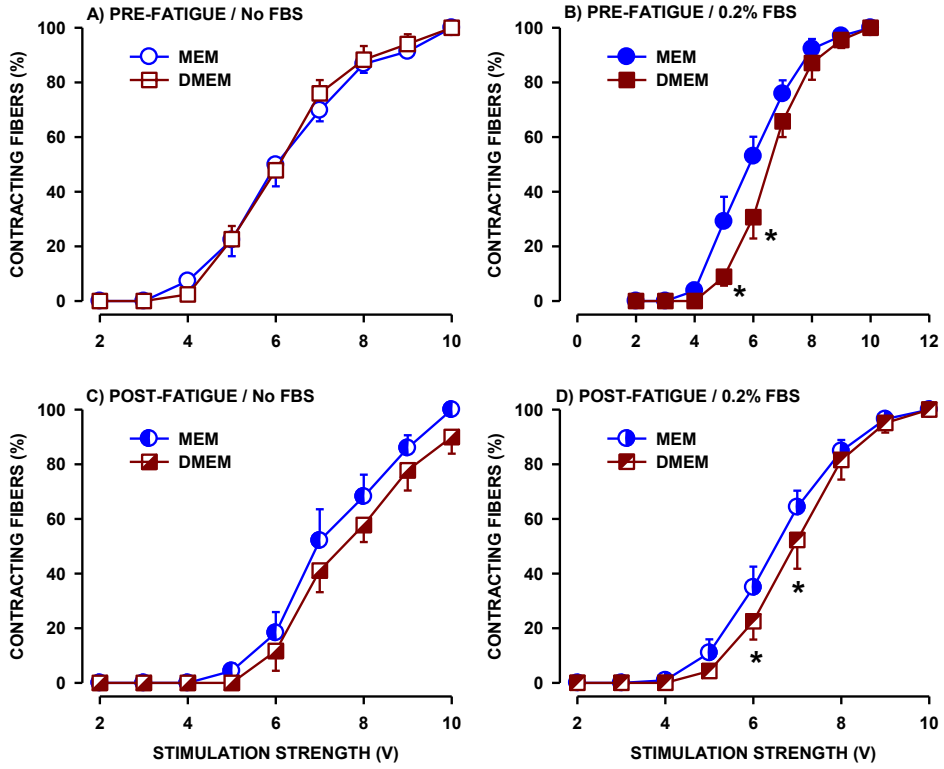

Figure 3.3. Effect of culture media on the contraction threshold of FDB single fibres. Single fibres were separated after a 3-hr digestion in 0.2% (w/v) collagenase in either MEM or DMEM culture media containing 10% (v/v) FBS. During measurements, fibres were superfused with physiological solution in the presence or absence of 0.2% FBS (v/v). Pre-fatigue measurements were performed after a 15 min equilibration period. Fatigue was elicited with one 200 msec long train of 10 V pulses at 120 Hz every sec for three minutes. Post-fatigue measurements were performed after a 10 min recovery period. Numbers of fibres are expressed as a percentage of the total number of contracting fibres at 10 V. Vertical bars represent the S.E. of 124-164 fibres from 5-8 mice.

* Marks a significant difference between MEM and DMEM as culture medium. ANOVA L.S.D., $P < 0.05$.

Figure 3.4

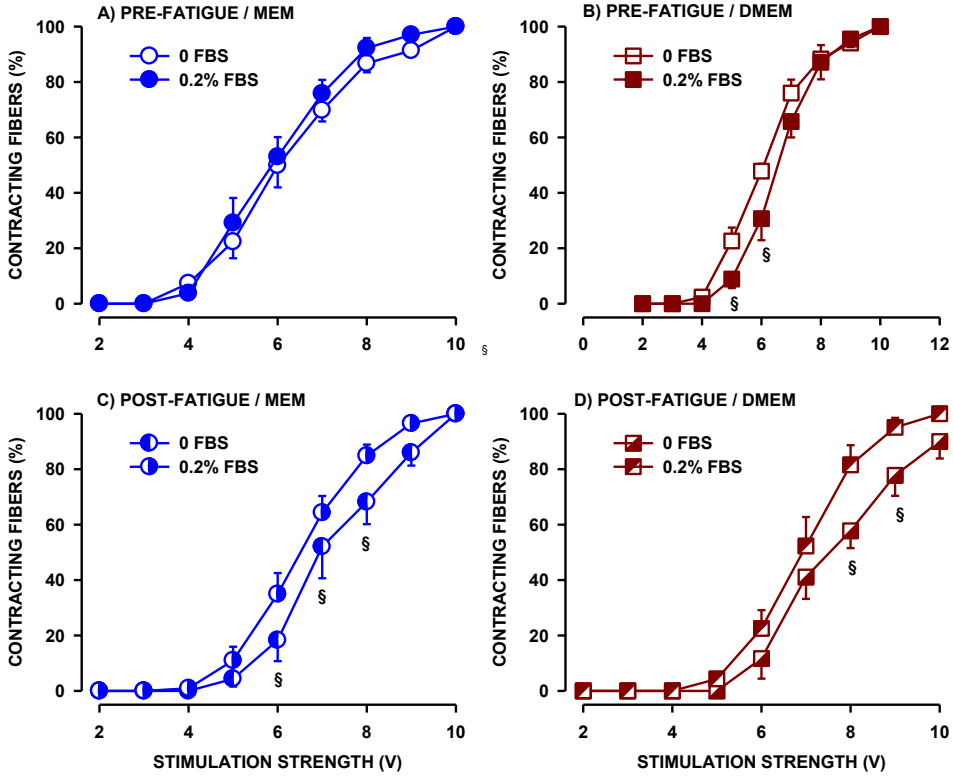

Figure 3.4. Effects of 0.2% FBS in the physiological solution on the contraction threshold of FDB single fibres. Single fibres were separated after a 3-hr digestion in 0.2% (w/v) collagenase in either MEM or DMEM culture media containing 10% (v/v) FBS. During measurements, fibres were superfused with physiological solution in the presence or absence of 0.2% FBS (v/v). Pre-fatigue measurements were performed after a 15 min equilibration period. Fatigue was elicited with one 200 msec long train of 10 V pulses at 120 Hz every sec for three minutes. Post-fatigue measurements were performed after a 10 min recovery period. Numbers of fibres are expressed as a percentage of the total number of contracting fibres at 10 V. Vertical bars represent the S.E. of 124-164 fibres from 5-8 mice. **§** Marks a significant difference between fibres superfused in physiological solution in the presence of absence of 0.2% (w/v) FBS. ANOVA L.S.D., $P < 0.05$.

Figure 3.5

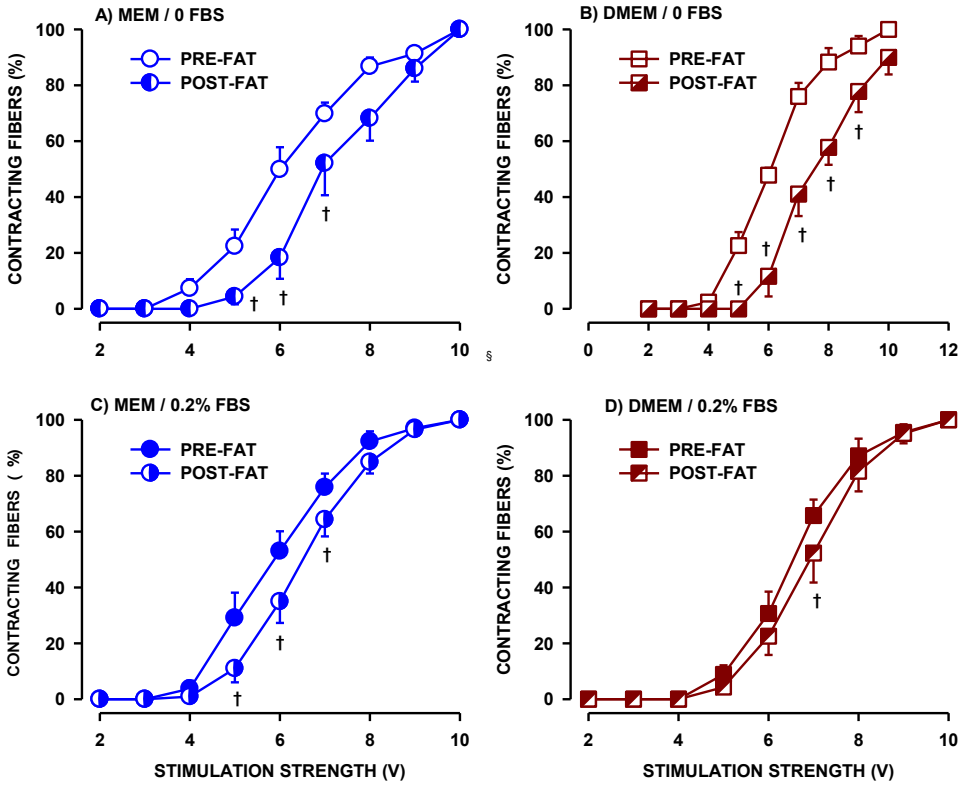

Figure 3.5. Effects of fatigue on contractility of FDB single fibres. Single fibres were separated after a 3-hr digestion in 0.2% (w/v) collagenase in either MEM or DMEM culture media containing 10% (v/v) FBS. During measurements, fibres were superfused with physiological solution in the presence or absence of 0.2% FBS (v/v). Pre-fatigue measurements were performed after a 15 min equilibration period. Fatigue was elicited with one 200 msec long train of 10 V pulses at 120 Hz every sec for three minutes. Post-fatigue measurements were performed after a 10 min recovery period. Numbers of fibres are expressed as a percentage of the total number of contracting fibres at 10 V. Vertical bars represent the S.E. of 124-164 fibres from 5-8 mice.

§ Marks a significant difference between the number of fibres contracting before or after fatigue was elicited. ANOVA L.S.D., $P < 0.05$.

When fibres were prepared in MEM and transferred to microscope chamber and superfused with physiological solution without FBS, the minimum voltage that resulted in fibres contracting was 4 V, and these fibres represented 7% of all contracting fibres at 10 V (Fig. 3.3A). Half of the fibres were contracting at stimulation strength of 6V. The relationship between the number of contracting fibres and stimulation strength for fibres prepared in DMEM was similar to that of fibres prepared in MEM. However, when 0.2% FBS was present in the physiological solution, FDB fibres prepared in MEM had lower thresholds than those prepared in DMEM (Fig. 3.3B). Following fatigue and recovery, fibres prepared in MEM had lower threshold than those in DMEM, with significant differences when 0.2% FBS was present (Fig. 3.3C, 3.5D).

For unfatigued fibres, the presence of 0.2% FBS in the physiological solution had no effect on contraction threshold for fibres prepared in MEM (Fig. 3.4A). Interestingly, the addition of 0.2% FBS to the physiological solution significantly increased the threshold for fibres prepared in DMEM (Fig. 3.4B). Following fatigue and recovery, thresholds were significantly lower in the presence of 0.2% FBS than they were in the absence of 0.2% FBS (Fig. 3.4C, 3.5D).

Fatigue is a reversible process, and consequently contraction threshold should be the same before and after fatigue once fibres have recovered. In the absence of FBS in the physiological solution, threshold values were significantly higher after fatigue for fibres prepared in MEM or DMEM (Fig. 3.5A, 3.5B). The presence of 0.2% FBS reduced this fatigue effect in both preparations (Fig. 3.5C, 3.5D).

From these results, it is clear that a collagenase digestion in MEM resulted in fibres with better morphology and contractile properties. The presence of 0.2% FBS in the physiological solution during experiments also improved fibre morphology and contractility, especially after fatigue is elicited. So, for the remainder of the study, fibre isolation (i.e. collagenase digestion) was performed using MEM culture medium containing 10% FBS, and all contractile measurements were performed with physiological solution containing 0.2% FBS.

Stability of fibre preparation

Effect of changing temperature

While fibres were kept in an incubator at 37°C until studied, their transfer to a cover slip and holding chamber always brought the temperature to approximately 22°C. Consequently, before any measurements could be performed the temperature had to be raised back to 37°C. During initial attempts to raise temperature to 37°C, it was noted that setting the experimental temperature on the heating apparatus to 37°C resulted in a temperature increase from 22-37°C in just 2-3 minutes. This rapid heating rate had a negative effect on contraction threshold of fibres, causing a shift of the threshold curve towards higher voltages, as temperature was raised to 37°C (Fig. 3.6A). When a more gradual approach to heating the fibres was taken, i.e. at a rate of 2°C every 100 s, the shift in threshold was no longer observed (Fig. 3.6B). It should also be noted that by the time these experiments were performed, more fibres were contracting, i.e. 78% compared to 59% in earlier experiments.

Figure 3.6

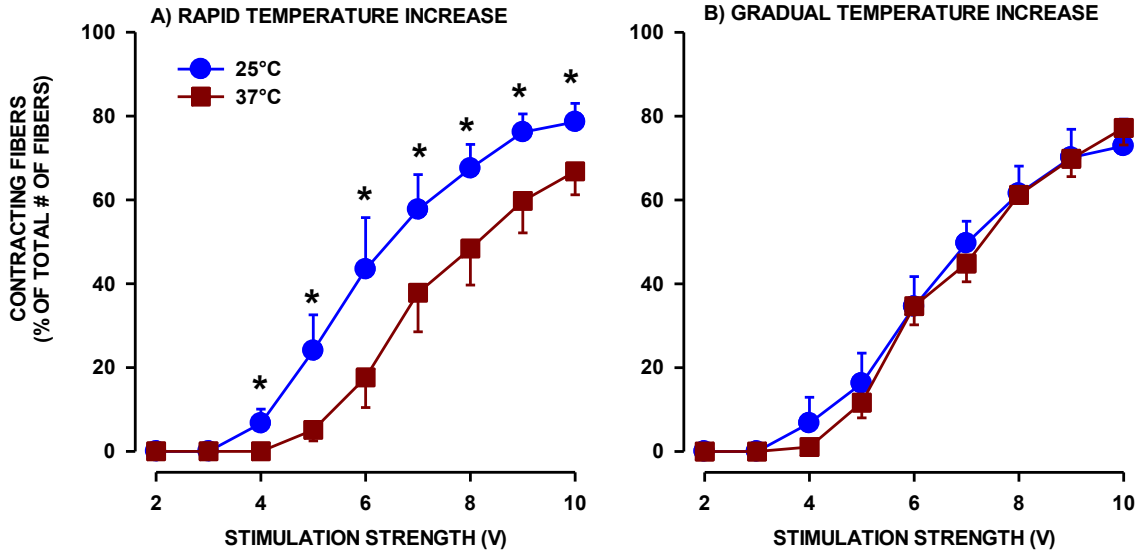

Figure 3.6. A rapid increase in experimental temperature from 25°C to 37°C was detrimental to FDB single fibres. Single fibres were separated after a 3-hr digestion in 0.2% (w/v) collagenase in MEM culture medium containing 10% (v/v) FBS. During measurements, fibres were superfused with physiological solution in the presence of 0.2% FBS (v/v). Numbers of fibres at different stimulus strengths are expressed as a percentage of the total number of contracting fibres at 10 V. The first measurement was at 25°C after a 15 min equilibration period. Temperature was increased from 25° to 37°C rapidly within 2 min (A) or gradually at a rate of 2° every 100 sec (B), and measurements were repeated. Stimulation consisted of 200 ms train of pulses at 120 Hz. Vertical bars represent the S.E. of 290-312 fibres from 3 mice.

* Marks a significant difference in the percentage of contracting fibres between 25°C and 37°C. ANOVA L.S.D., $P < 0.05$.

Stability over time

The next factor to be studied was the window of time during which an experiment can run without the loss of fibre viability. In a previous study (Cifelli *et al.*, 2007), fibres had been used for an experiment the day after they had been prepared. In this study, when fibres were tested the day they were prepared (day 0), the number of contracting fibres at 25°C was 80% and did not change after the temperature was raised from 25° to 37°C (Fig. 3.7A). Furthermore, fibres remained stable for up to 3 hours; i.e., with no loss in contractility. When fibres were tested the day after they were prepared (day 1), there was a loss in the proportion of contracting fibres immediately following the increase in temperature from 25-37°C, from 80% to 71% (Fig. 3.7B). Moreover, a continual loss of contracting fibres was observed over time. There was also no change in fibre contraction threshold as a result of heating from 25-37°C, or over the three-hour period at 37°C (Fig. 3.8A). There were, however, significant shifts towards higher voltage thresholds for fibres studied 1 day after preparation (Fig. 3.8B). These results suggest that although there are still contracting fibres on day 1, the fibre preparation is not as reliable as it is on day 0. For consistent results, and for the remainder of this study, all fibres were used the day they were prepared.

Sarcomere shortening

Shortening-frequency curve

The higher the frequency of stimulation, the more force a muscle can produce. Since there is no tendon left after a collagenase digestion, it was not possible to measure force in this study. Instead, the shortening-frequency relationship was measured and we tested

Figure 3.7

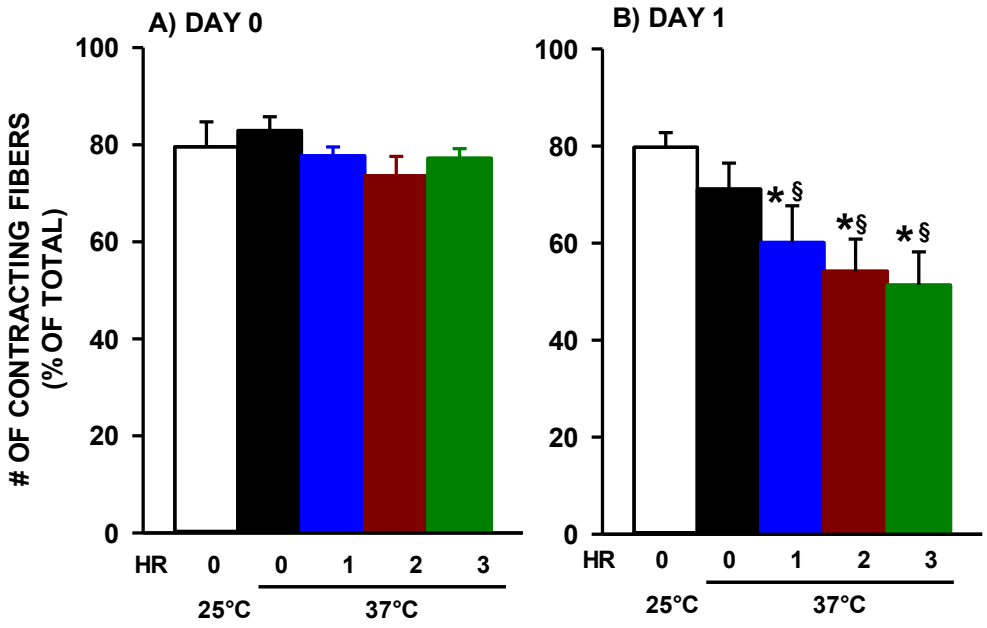

Figure 3.7. FDB single fibres are stable for 3 hours when tested the day of the preparation. Single fibres were separated after a 3-hr digestion in 0.2% (w/v) collagenase in MEM or culture medium containing 10% (v/v) FBS. Fibres were tested immediately following the 3-hr incubation (A) or were left incubating overnight (≈24 hours) and then tested (B). During measurements, fibres were superfused with physiological solution containing 0.2% FBS (v/v). Numbers of contracting fibres are expressed as the total number of contracting fibres. They were first determined at 25°C after a 15 min equilibration period, immediately after reaching 37°C, and every hour thereafter. Fibres were stimulated every 100 sec throughout the 3 hour experimental period with 200 ms train of 10 V pulses at 120 Hz. Vertical bars represent the S.E. of 251-265 fibres from 7 mice.

* Marks a significant difference between day 0 and 1 in the number of contracting fibres.

§ Marks a significant difference in the number of contracting fibres when compared to the data at 25°C. ANOVA L.S.D., $P < 0.05$.

Figure 3.8

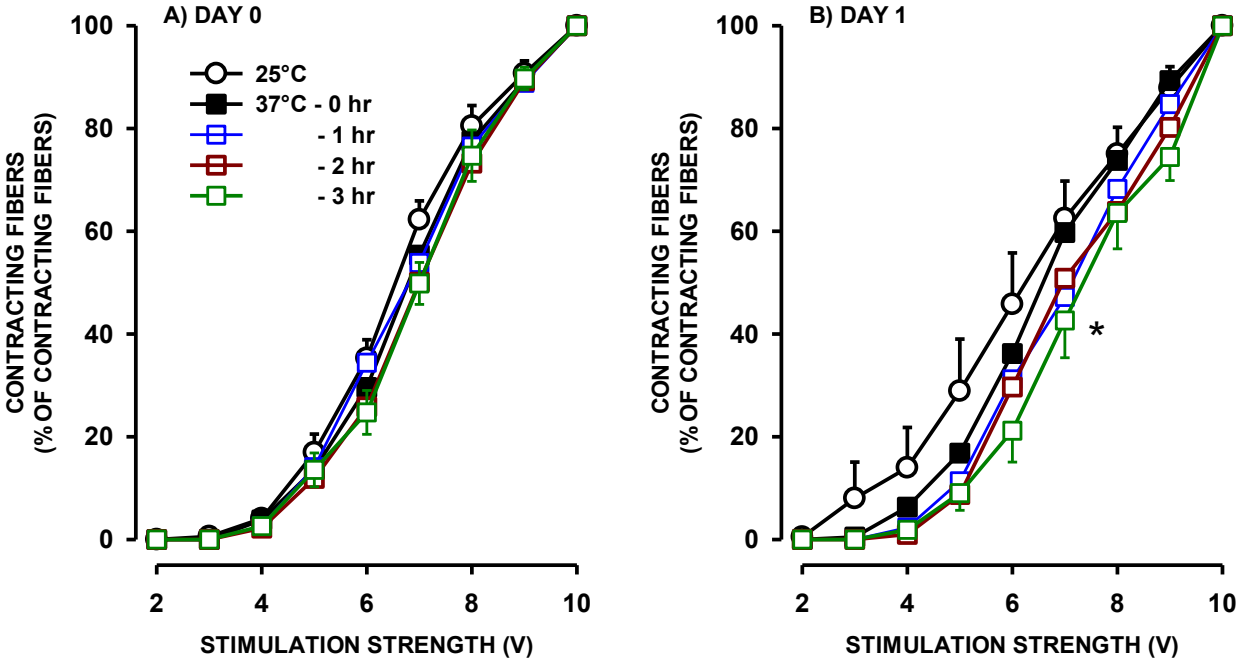

Figure 3.8. Contractility of FDB single fibres was stable for 3 hours when tested the day of the preparation. Single fibres were separated after a 3-hr digestion in 0.2% (w/v) collagenase in MEM culture medium containing 10% (v/v) FBS. Fibres were tested A) the day they were separated or B) after 24 hours of incubation at 37°C in MEM. During measurements, fibres were superfused with physiological solution containing 0.2% FBS (v/v). Number of contracting fibres is expressed as a percent of total number of contracting fibres at 10 V. They were first determined at 25°C after a 15 min equilibration period, immediately after reaching 37°C, and every hour thereafter. Fibres were stimulated every 100 sec throughout the 3 hour experimental period with 200 ms train of 10 V pulses at 120 Hz. Vertical bars represent the S.E. of 251-265 fibres from 7 mice.

* Marks a significant difference in the number of contracting fibres when compared to the data at 25°C. ANOVA L.S.D., $P < 0.05$.

whether the curve is shifted toward higher frequency as temperature is increased, as is observed for force.

Figure 3.9 shows sarcomere shortening in single fibres elicited at different frequencies. At 25°C, the 10 Hz stimulation resulted in small unfused twitches (Fig. 3.9A). As the frequency of stimulation was increased, the extent of shortening increased. The same situation was observed at 37°C (Fig. 3.9B). At 37°C, twitches at 10 Hz were sharper with more discreet peaks than at 25°C. Fusion of twitch contractions at 30-50 Hz was also less evident at 37°C than at 25°C (Fig. 3.9C). From 10-80 Hz, shortenings at 25°C were significantly greater than at 37°C. At 100 Hz, shortening was the same at 25°C or 37°C.

Sarcomere shortening during fatigue

Changes in resting sarcomere length and shortening capacity during fatigue were measured in FDB single fibres. Prior to fatigue, resting length was 1.88 μm. During the first tetanic contraction elicited by a 200 ms pulse at 100 Hz, the sarcomere length was observed to decrease to 1.37 μm, representing a shortening of 0.50 μm. Throughout the fatigue protocol, resting length diminished from 1.88 μm to 1.72 μm as repetitive contractions were elicited. Contracted length due to stimulation decreased initially from 1.37 μm to 1.29 μm by time t = 60s, before increasing to 1.55 μm at the end of the fatigue simulation at time t = 180s (Fig. 3.10). These contracted lengths throughout fatigue translate to a decreased shortening as fatigue progresses, going from an initial shortening of 0.50 μm as a result of the first contraction, to 0.17 μm at 180 s. After a 10-minute recovery period, there was a recovery of 99% in resting sarcomere length back to pre-fatigue levels, only a 4% increase in length at

Figure 3.9

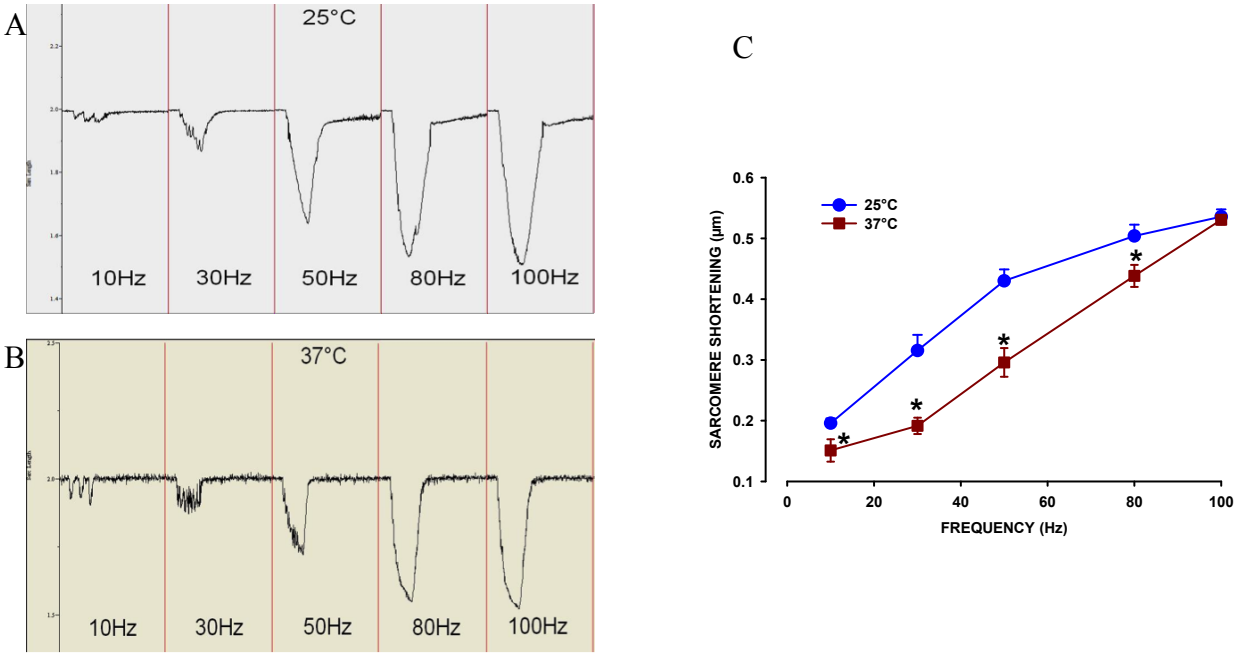

Figure 3.9. Effect of increasing temperature on the sarcomere shortening-stimulation frequency relationship. When the experimental temperature was increased from 25° to 37°C, the relationship was shifted to higher frequencies. Stimulation strength was 10 V. Examples of sarcomere shortening traces at various frequencies at 25°C (A) and at 37°C (B). C) Shortening-frequency relationship. Vertical bars represent the S.E. for 42-102 fibres from 5-8 mice.

* Marks a significant difference between 25°C and 37°C for a given frequency of stimulation. ANOVA L.S.D., $P < 0.05$.

the peak of contraction, and a recovery of 86% in total shortening capacity (difference between resting sarcomere length and contracted sarcomere length).

Final protocol for isolation of viable single fibres

The experiments performed resulted in a working protocol to yield an increased number of viable contracting fibres. This represents an advance over current methodology. The final protocol involves a 3 hour collagenase digestion of FDB muscles in MEM culture medium containing 10% FBS. The fibres are then placed on glass coverslips covered with a thin coat of Matrigel™. After mounting the coverslip into a chamber, single FDB fibres are superfused with physiological solution containing 0.2% FBS. Under these conditions, fibres are stable for at least 3 hours when tested on the day of dissociation.

Figure 3.10

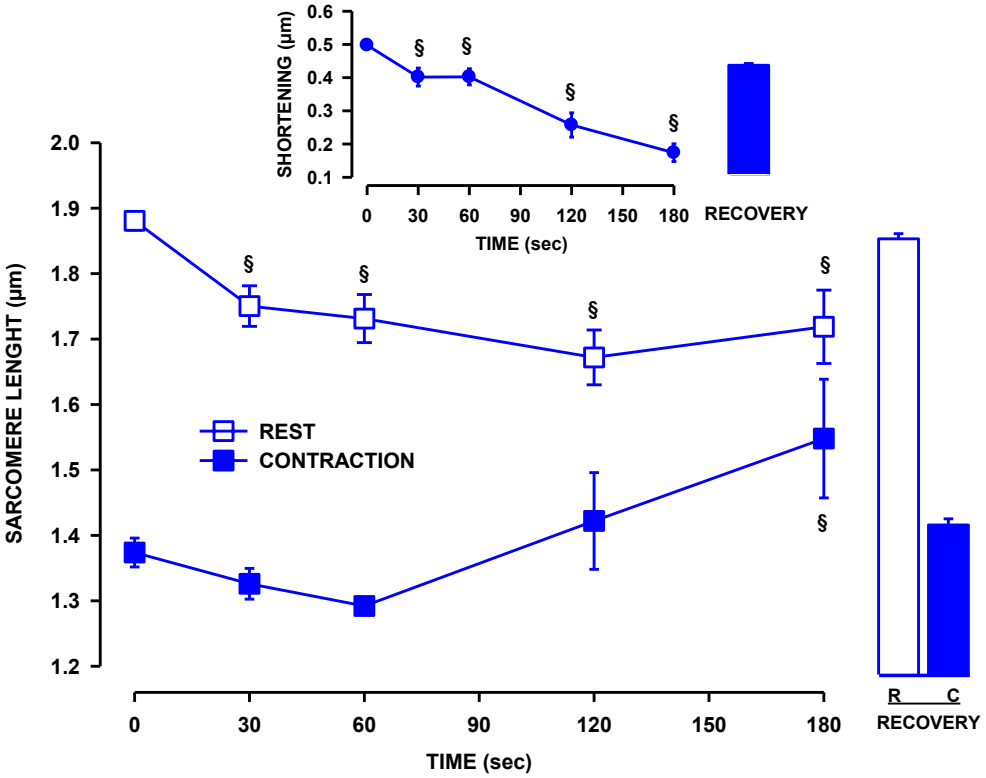

Figure 3.10. FDB single fibres recovered shortening-capacity within 10 min after a fatigue stimulation. Single fibres were separated after a 3-hr digestion in 0.2% (w/v) collagenase in MEM culture medium containing 10% (v/v) FBS. During measurements, fibres were superfused with physiological solution containing 0.2% FBS (v/v). Fatigue was elicited with one 200 ms tetanic contraction every second for 180 s. For the fatigue period, chang4es in sarcomere lengths are shown every 30 sec. Sarcomere lengths were also measured after a 10 min recovery period during which fibres were stimulated once every 100 s. Shortening length is the difference between resting length and contracted length. Vertical bars represent S.E. of 6-10 fibres from 4-6 mice.

§ Marks a significant difference between the sarcomere length at any given time and sarcomere length at rest (time t = 0 s). ANOVA L.S.D., $P < 0.05$.

Effects of verapamil and NAC on fatigue kinetics in K_{ATP} channel deficient FDB fibres

The main goal of this study was to determine the nature of the elevated unstimulated $[Ca^{2+}]_i$ observed in K_{ATP} channel deficient FDB fibres undergoing a fatigue protocol. Indirect evidence had been obtained in which a small dose of verapamil prevented the large increase in unstimulated force during fatigue, suggesting that it is linked to an elevated Ca^{2+} influx through L-type Ca^{2+} channels (Cifelli *et al.*, 2008). It has been recently shown, using ROS scavengers, that ROS may also play a role in this elevated unstimulated force, perhaps by affecting $[Ca^{2+}]_i$ (Gariepy-Boudreault, 2010). Therefore, it was proposed to determine how a partial blockage of L-type Ca^{2+} channels by verapamil and how NAC, a ROS scavenger, affect $[Ca^{2+}]_i$ during fatigue in K_{ATP} channel deficient fibres.

Two models for K_{ATP} channel deficiency were used: (1) glibenclamide was used as a pharmacological approach to block K_{ATP} channel activity in wild type fibres, and (2) knockout mice for the Kir6.2 gene were used because these FDB fibres do not express functional K_{ATP} channels. Myoplasmic Ca^{2+} was measured using Fura-2, a fluorescent indicator. While changes in sarcomere shortening during fatigue were shown in Figure 3.10, this measurement was very difficult because any slight displacements of the fibre during repeated contractions and fatigue caused loss of focus. These displacements made the Fourier analysis impossible for many fibres. To avoid eliminating many fibres, and to maintain a large enough fibre population, only $[Ca^{2+}]_i$ was measured for this study.

Unstimulated $[Ca^{2+}]_i$

Unstimulated $[Ca^{2+}]_i$ is the $[Ca^{2+}]_i$ that is measured 100 msec before a contraction is elicited. In this section, unstimulated $[Ca^{2+}]_i$ is first examined as an average of all fibres tested in a particular group, so as to be able to compare with previous results in whole muscle.

Prior to fatigue, mean unstimulated $[Ca^{2+}]_i$ in wild type control fibres was 20.2 nM (Fig. 3.11A). During fatigue, unstimulated $[Ca^{2+}]_i$ gradually increased to 137.6 nM by 85 s, and slightly declined thereafter reaching a value of 102.5 nM by 180 s, still above pre-fatigue levels.

For wild type fibres exposed to 10 μM glibenclamide, unstimulated $[Ca^{2+}]_i$ increased sharply within 10 sec from 38.1 nM to 175.2 nM at 10 s. It then continued to increase at a slower rate, reaching 234 nM at 65 s, before decreasing to 96.3 nM by the end of fatigue. The unstimulated $[Ca^{2+}]_i$ was much higher for glibenclamide-exposed wild type fibres, than it was for wild type control fibres.

A similar sharp increase in unstimulated $[Ca^{2+}]_i$ was not observed in the other model of K_{ATP} channel deficiency. For Kir6.2$^{-/-}$ fibres, unstimulated $[Ca^{2+}]_i$ increased even more slowly than it did in wild type control, from 14.2 nM to 122.5 nM in 95 sec. Thereafter, the unstimulated $[Ca^{2+}]_i$ was similar to that of wild type control.

The changes in unstimulated $[Ca^{2+}]_i$ were the same for fibres that were concomitantly exposed to glibenclamide and either verapamil or NAC. Furthermore, the increases were significantly less than those fibres exposed only to glibenclamide (Fig. 3.11B).

Figure 3.11

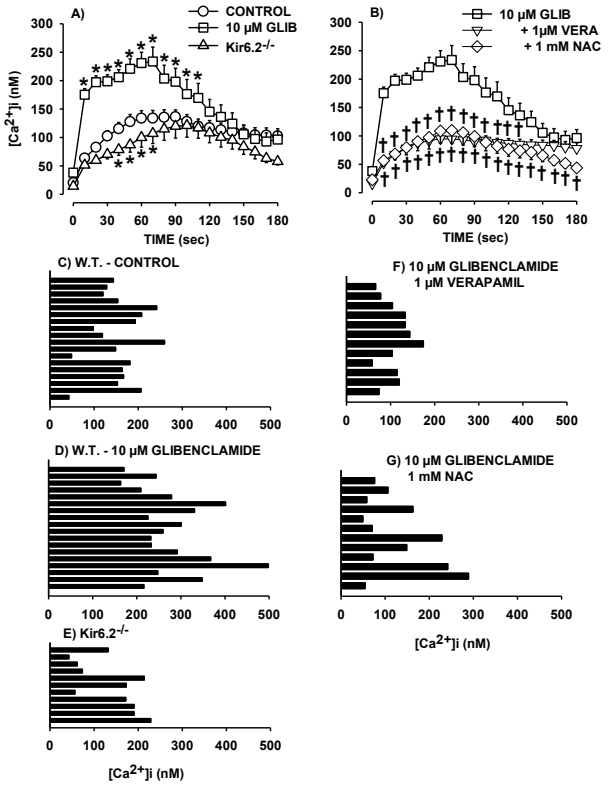

Figure 3.11. Effects of verapamil or NAC on the unstimulated $[Ca^{2+}]_i$ observed during fatigue in glibenclamide-exposed FDB single fibres. Fatigue was elicited with one 200 ms long tetanic contraction (100 Hz) every sec for 3 min. A) Effect of no K_{ATP} channel on unstimulated $[Ca^{2+}]_i$. B) Effect of verapamil and NAC on unstimulated $[Ca^{2+}]_i$ in glibenclamide-exposed fibres. C-G) Maximum unstimulated $[Ca^{2+}]_i$ for each individual fibre that was measured during the fatigue period. The fibre order are from the most (top horizontal bar) to the least (bottom horizontal bar) fatigue resistant as determined from the decrease in tetanic $[Ca^{2+}]_i$ as shown in Figures 3-13 to 3.17 for each experimental conditions.

§ Marks a significant difference from time 0.

* Marks a significant difference from wild type control fibres.

† Marks a significant difference from glibenclamide-exposed wild type fibres. Vertical bars represent S.E. of 11-18 fibres from 4-6 mice. ANOVA L.S.D., $P < 0.05$.

FDB expressed myosin I, IIA, and IIX isoforms giving rise to the fibre types listed in Table 3.1. In general, fatigue resistance is in the order of I ~ IIA > IIX (Larsson *et al.*, 1991). It was therefore not surprising to observe large differences in fatigue kinetics between fibres. Here, differences in unstimulated $[Ca^{2+}]_i$ between fibres was examined, and later tetanic $[Ca^{2+}]_i$ will be examined.

Fibre Type	Content
I	2%
I-IIA	6%
I-IIX	8%
IIA	19%
IIA-IIX	32%
IIX	21%
I-IIA-IIX	9%
Other	3%

Table 3.1: Fibre Type Composition of FDB Muscle (Reproduced from Banas, 2011).

Thirteen of 18 wild type control fibres had maximum unstimulated $[Ca^{2+}]_i$ levels of 120 nM or higher, while only two fibres reached unstimulated $[Ca^{2+}]_i$ levels 240 nM (Fig. 3.11C). All 18 glibenclamide-exposed wild type fibres reached unstimulated $[Ca^{2+}]_i$ levels of 120 nM or higher, while 11 out of 18 surpassed unstimulated $[Ca^{2+}]_i$ levels 240 nM (Fig. 3.11D). Seven of 11 Kir6.2$^{-/-}$ fibres had unstimulated $[Ca^{2+}]_i$ increase to 120 nM or above, with none reaching 240 nM (Fig. 3.11E). For fibres exposed to glibenclamide and verapamil, only two of 12 fibres reached unstimulated $[Ca^{2+}]_i$ levels of 120 nM with none reaching 240 nM (Fig. 3.11F). For the NAC and glibenclamide condition, five of 12 fibres reached unstimulated $[Ca^{2+}]_i$ of 120 nM and of these fibres, only two reached 240nM (Fig. 3.11G). Unstimulated $[Ca^{2+}]_i$ does not seem to be related to variability in fatigue resistance between individual single FDB fibres.

Tetanic $[Ca^{2+}]_i$

Before fatigue (1st contraction in Fig. 3.12A), mean tetanic $[Ca^{2+}]_i$, which was the average of $[Ca^{2+}]_i$ values measured at peak of contraction, within wild type control fibres, was 1.2 μM. During the fatigue stimulation, tetanic $[Ca^{2+}]_i$ first increased to

Figure 3.12

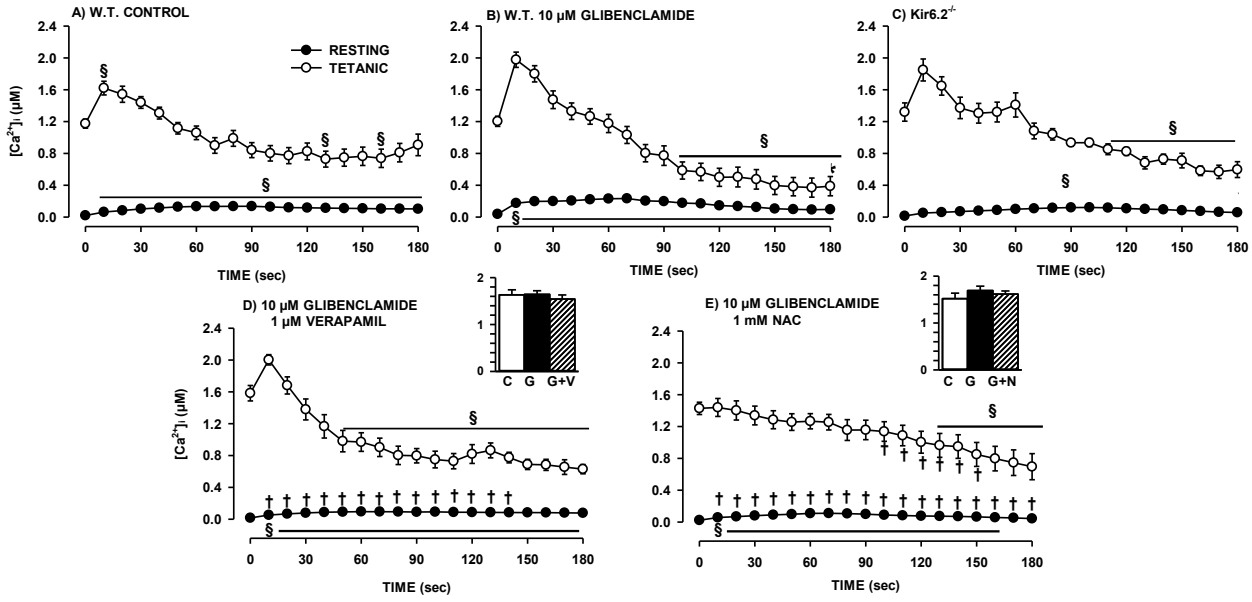

Figure 3.12. Effects of no KATP channel activity, verapamil and NAC on tetanic $[Ca^{2+}]_i$. Fatigue was elicited with one 200 ms long tetanic contraction (100 Hz) every sec for 3 min. Resting $[Ca^{2+}]_i$ was measured between contractions while tetanic $[Ca^{2+}]_i$ was measured during the plateau phase when fibres were elicited to contract. Insets show the effects of glibenclamide (G), verapamil (V), and NAC (N) on $[Ca^{2+}]_i$ prior to fatigue. Adding glibenclamide, verapamil, or NAC to control fibres (C) had little to no effect on $[Ca^{2+}]_i$ prior to fatigue.

§ Marks a significant difference from time 0.

* Marks a significant difference from control.

† Marks a significant difference from glibenclamide-exposed wild type control.

Vertical bars represent S.E. of 11-18 fibres from 4-6 mice. ANOVA L.S.D., $P < 0.05$.

1.64 μM by 15 s, then decreased gradually to 0.81 μM at 170 s finishing with a tetanic $[Ca^{2+}]_i$ value of 0.91 μM at 180 s. Initial mean tetanic $[Ca^{2+}]_i$ values for unfatigued glibenclamide-exposed fibres were the same as those of wild type control fibres (Fig. 3.12B), but increased more during the first 10 sec reaching 1.98 μM compared to 1.64 μM for control. The subsequent decrease was then greater for glibenclamide-exposed fibres becoming significantly different by 100 sec, reaching a minimum tetanic $[Ca^{2+}]_i$ value of 0.36 μM compared to 0.73 μM for wild type control fibres.

Compared to wild type control and glibenclamide-exposed wild type fibres, mean tetanic $[Ca^{2+}]_i$ values for Kir6.2$^{-/-}$ fibres were not significantly higher with an average value of 1.32 μM (Fig. 3.12C). Tetanic $[Ca^{2+}]_i$ rapidly increased to 1.85 μM by 10 s, then decreased to 0.60 μM (end of fatigue). The decrease in tetanic $[Ca^{2+}]_i$ for wild type control, wild type fibres exposed to glibenclamide, and Kir6.2$^{-/-}$ fibres with fatigue were 45%, 80%, and 68 % respectively.

Verapamil barely altered the kinetics of the tetanic $[Ca^{2+}]_i$ changes during fatigue. The 69% decrease in tetanic $[Ca^{2+}]_i$ observed in fibres exposed to both glibenclamide and verapamil was larger than the decrease observed in wild type control fibres but smaller than the decrease observed in fibres that were exposed to glibenclamide alone (Fig. 3.12D). NAC, on the other hand, had a pronounced effect on tetanic $[Ca^{2+}]_i$ (Fig. 3.12E). With the addition of NAC to glibenclamide-exposed fibres, the initial increase in tetanic $[Ca^{2+}]_i$, observed under all other conditions, was abolished. Also, the decrease in tetanic $[Ca^{2+}]_i$ that occurred during fatigue was linear, whereas the decrease observed under other conditions was exponential.

Differences in fatigue kinetics between fibres

Wild type control FDB fibres

Of the 18 fibres tested, six had higher tetanic $[Ca^{2+}]_i$ at the end than at the beginning of the fatigue period. Two fibres had decreases that were less than 10% (3.13A). These eight fatigue resistant fibres made up group C1. Averaging tetanic $[Ca^{2+}]_i$ for these eight fibres showed a starting tetanic $[Ca^{2+}]_i$ of 1.19 μM, and a final tetanic $[Ca^{2+}]_i$ of 1.41 μM (18% increase).

The second and third wild type control groups, C2 and C3, were characterized by significant decreases in tetanic $[Ca^{2+}]_i$ (Fig. 3.13C,D). Group C3 consisted of the five least fatigue resistant fibres, and the decline in tetanic $[Ca^{2+}]_i$ was greatest in this group and became significant before 60 s reaching a minimum mean tetanic $[Ca^{2+}]_i$ value of only 0.23 μM at 160 s. Group C2 was made up of the five fibres that demonstrated intermediate decreases in tetanic $[Ca^{2+}]_i$, reaching plateau at a value of 0.70 μM after 90 sec. This is also the time when the decrease became significant in this group.

Wild type FDB fibres exposed to 10 μM glibenclamide

There were also FDB fibres exposed to 10 μM glibenclamide (G1) for which mean tetanic $[Ca^{2+}]_i$, at the end of fatigue, was either higher (two fibres) or less than (two fibres) 15% lower than pre-fatigue levels (Fig. 3.14B). For group G1, the initial mean tetanic $[Ca^{2+}]_i$ was 1.12 μM, and the final tetanic $[Ca^{2+}]_i$ after fatigue was 1.19 μM (6% increase with fatigue). For all 14 other fibres, the decreases in tetanic $[Ca^{2+}]_i$ were very large. Three distinct patterns were observed. For some fibres grouped together as G2

Figure 3.13

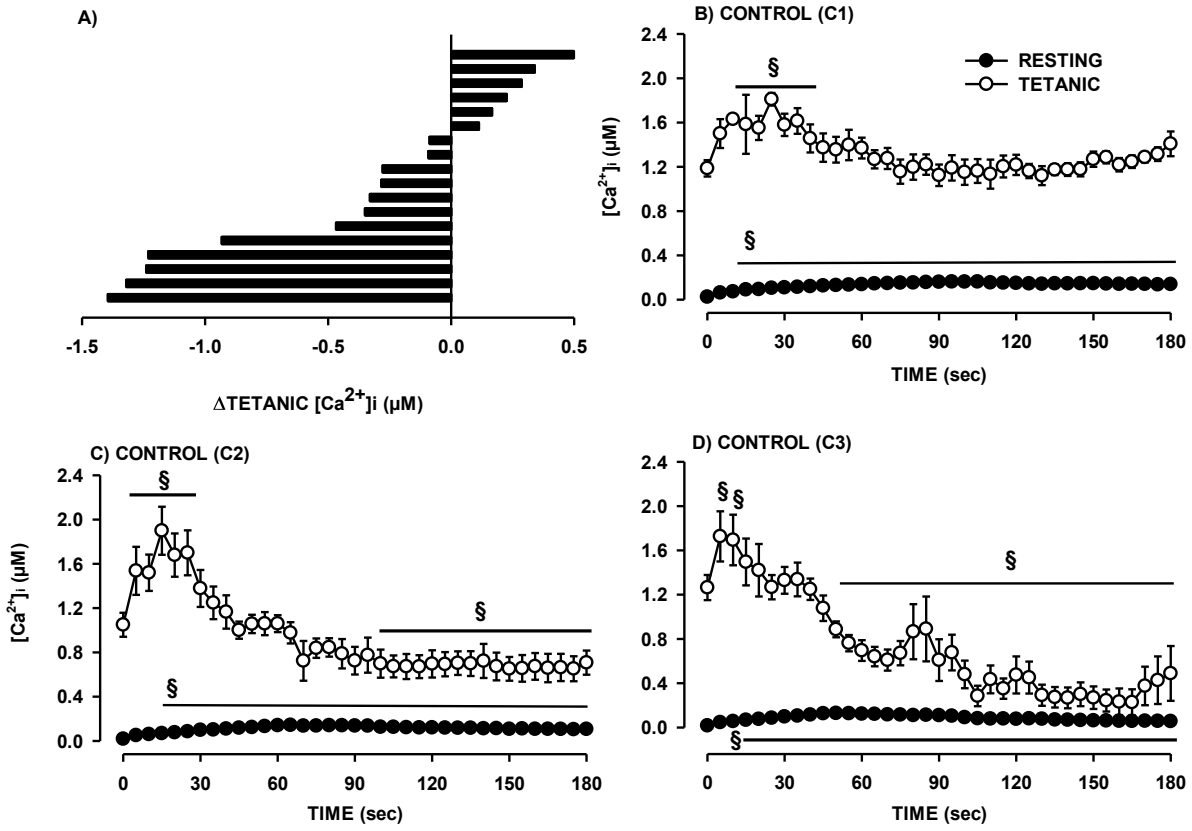

Figure 3.13. Fatigue kinetics of individual wild type FDB single fibres in control conditions. Fatigue was elicited with one 200 ms long tetanic contraction (100 Hz) every sec for 3 min. A) Magnitudes of the changes in tetanic $[Ca^{2+}]_i$ for individual wild type control fibres calculated as the difference in tetanic $[Ca^{2+}]_i$ between time 0 and 180 sec. B) Group C1 consisted of fibres that had higher or less than a 10% decrease in tetanic $[Ca^{2+}]_i$ during fatigue (top 8 fibres in A). C) Group C2 consisted of fibres that had intermediate decreases in tetanic $[Ca^{2+}]_i$ (middle 5 fibres in A). D) Group C3 consisted of fibres that had in the largest decrease in tetanic $[Ca^{2+}]_i$ (bottom 5 fibres in A).

§ Marks a significant difference from time 0. ANOVA L.S.D., $P < 0.05$.

Figure 3.14

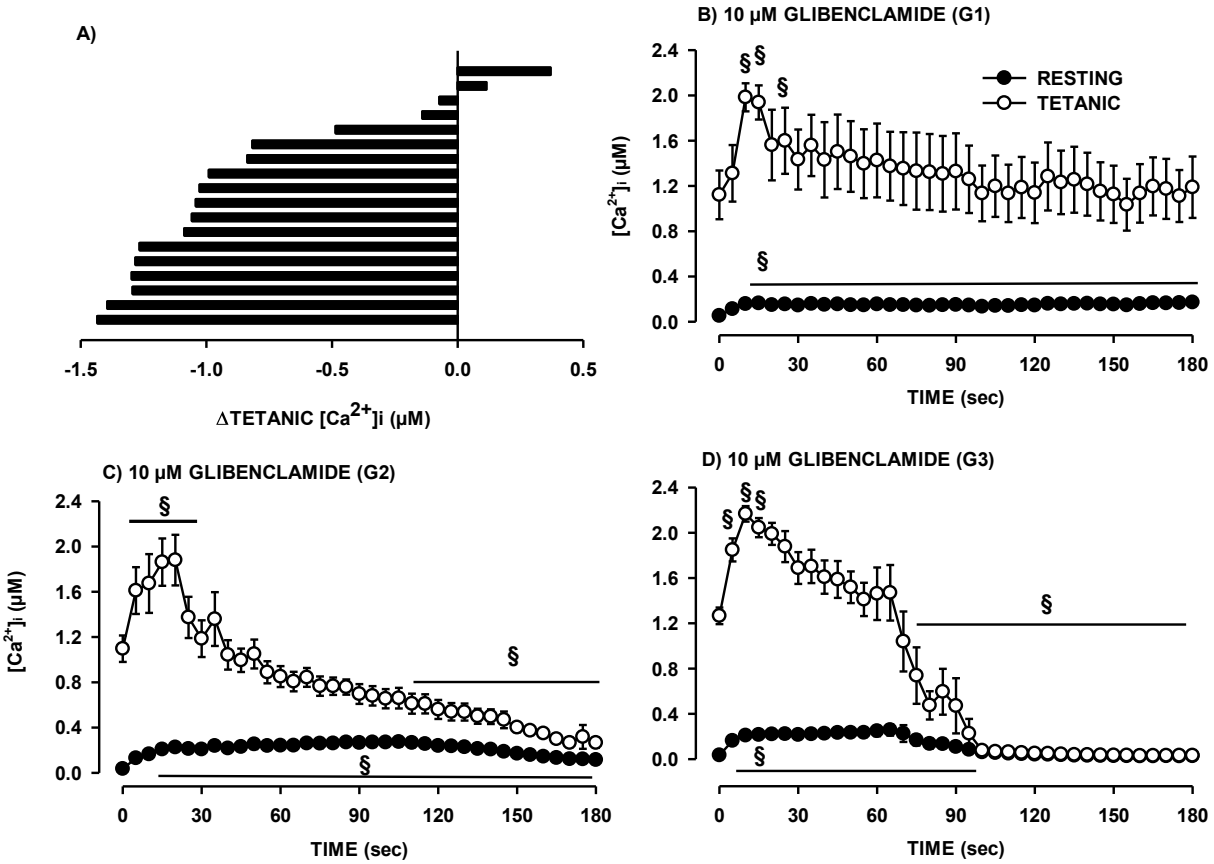

Figure 3.14. Fatigue kinetics of individual wild type FDB single fibres exposed to glibenclamide. Fatigue was elicited with one 200 ms long tetanic contraction (100 Hz) every sec for 3 min. A) Magnitudes of changes in tetanic $[Ca^{2+}]_i$ for individual glibenclamide-exposed wild type fibres. B) Group C1 consisted of fibres that had higher or less than a 15% decrease in tetanic $[Ca^{2+}]_i$ during fatigue (top 4 fibres in A). C) Group C2 consisted of fibres that had intermediate decreases in tetanic $[Ca^{2+}]_i$ (middle 5 fibres in A). D) Group C3 consisted of fibres that had in the largest decrease in tetanic $[Ca^{2+}]_i$ and a sudden and complete loss of contractility between 70 and 100 sec (5 of the bottom 9 fibres in A; the other 4 fibres also had a sudden and complete loss in contractility but after 120 sec, data not shown).

§ Marks a significant difference from time 0. ANOVA L.S.D., $P < 0.05$.

(middle five fibres), a large gradual decline in tetanic $[Ca^{2+}]_i$ occurred beginning at 30 sec through the end of fatigue (Fig. 3.14C). For the most fatigable fibres, some had a sudden and complete loss of contraction between 70 sec and 100 sec (group C3 = five fibres) as shown in Fig 3.14D. For the remaining four fibres, the sudden and complete loss of contractility occurred later (between 120 sec and 150 sec, data not shown).

Kir6.2$^{-/-}$ FDB fibres

For Kir6.2$^{-/-}$ fibres, only one of 11 fibres had more tetanic $[Ca^{2+}]_i$ at the end than at the beginning of the fatigue period (Fig. 3.15A). For the four most fatigue resistant fibres, group K1, starting tetanic $[Ca^{2+}]_i$ was 1.09 μM, and the final tetanic $[Ca^{2+}]_i$ after fatigue was 0.80 μM (mean 27% decrease with fatigue).

The second and third groups of Kir6.2$^{-/-}$ (K1 and K2) had larger and significant decreases in tetanic $[Ca^{2+}]_i$ (Fig. 3.15C,D). Before fatigue, K2 had an initial mean tetanic $[Ca^{2+}]_i$ value of 1.34 μM compared to 1.61 μM for K3. After the initial increase in $[Ca^{2+}]_i$ to 2.06 μM for K2, tetanic $[Ca^{2+}]_i$ remained constant for 20 sec before dropping significantly. For K3, there was no plateau. At the end of fatigue tetanic $[Ca^{2+}]_i$ for K2 and K3 were respectively 0.59 μM and 0.41 μM.

Wild type FDB fibres exposed to 10 μM glibenclamide and 1 μM verapamil

All FDB single fibres that were exposed to both glibenclamide and verapamil contracted successfully through the entire fatigue protocol. However, when the decrease in tetanic $[Ca^{2+}]_i$ for each fibre was plotted, the differences in $[Ca^{2+}]_i$ from the most fatigue resistant to the most fatigable fibres was a spectrum. Looking at individual traces

Figure 3.15

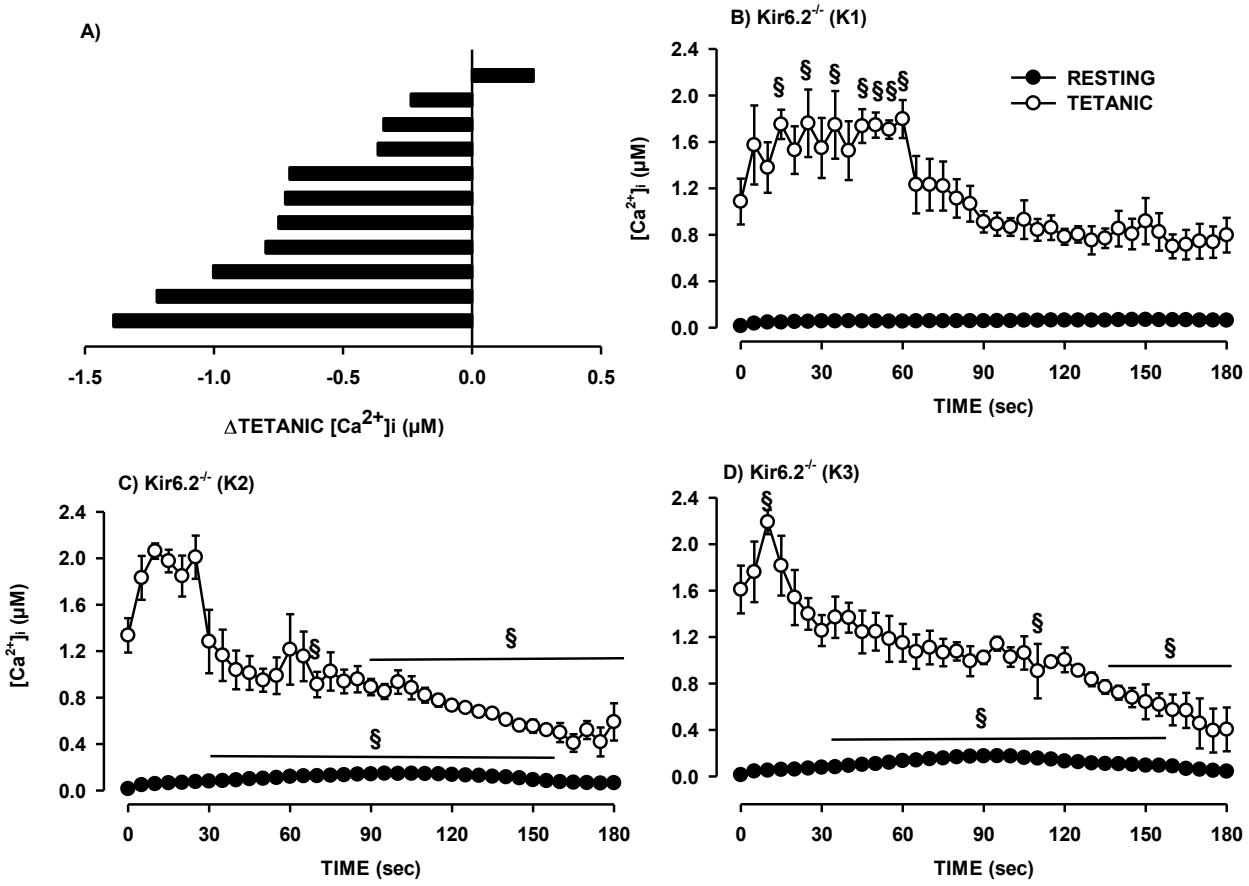

Figure 3.15. Fatigue kinetics of individual Kir6.2$^{-/-}$ FDB single fibres under control conditions. Fatigue was elicited with one 200 ms long tetanic contraction (100 Hz) every sec for 3 min. A) Magnitudes of changes in tetanic $[Ca^{2+}]_i$ for individual Kir6.2$^{-/-}$ fibres. B) Group K1 consisted of fibres that had no decrease or the smallest decrease in tetanic $[Ca^{2+}]_i$ (top 4 fibres in A). C) Group K2 consisted of fibres that had intermediate decreases in tetanic $[Ca^{2+}]_i$ (middle 4 fibres in A). D) Group K3 consisted of fibres that had the largest decrease in tetanic $[Ca^{2+}]_i$ (bottom 3 fibres in A).

§ Marks a significant difference from time 0. ANOVA L.S.D., $P < 0.05$.

demonstrated that for 3 fibres the decrease in tetanic $[Ca^{2+}]_i$ was gradual and continuous from 30-180 sec (Fig. 3.16B) whereas for the other nine there was a very large decrease between 10-50 sec (Fig. 3.16C).

Wild type FDB fibres exposed to 10 μM glibenclamide and 1 mM NAC

As observed with verapamil, the decrease in tetanic $[Ca^{2+}]_i$ for different fibres made up a spectrum. Figure 3.17B shows $[Ca^{2+}]_i$ for the first four fibres, whereas Figure 3.17C shows $[Ca^{2+}]_i$ for the other seven fibres. The first group of fibres, N1, was characterized by very small and gradual decreases in tetanic $[Ca^{2+}]_i$, whereas the other fibres exposed to both glibenclamide and NAC (group N2) did not experience steep reductions in tetanic $[Ca^{2+}]_i$. Decreases in tetanic $[Ca^{2+}]_i$ were much more gradual.

Figure 3.16

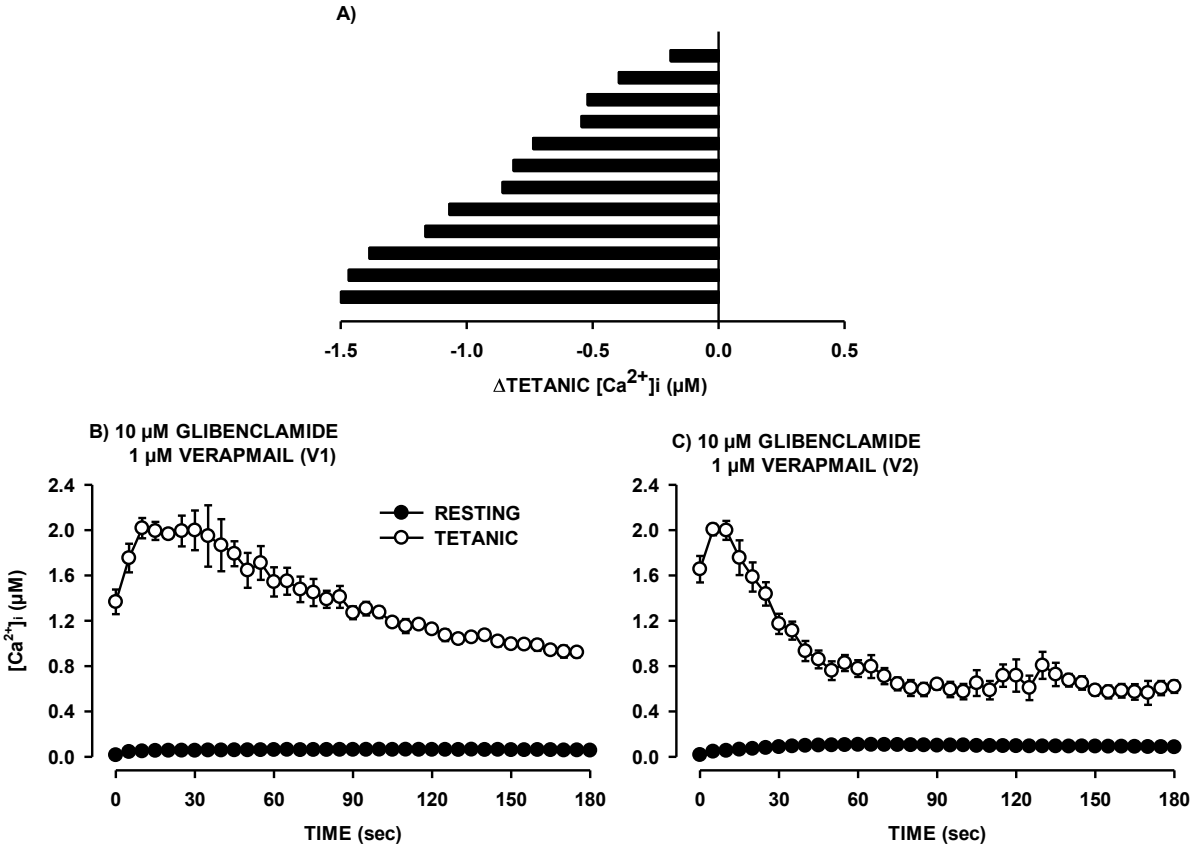

Figure 3.16. Fatigue kinetics of individual wild type FDB single fibres exposed to glibenclamide and verapamil. Fatigue was elicited with one 200 ms long tetanic contraction (100 Hz) every sec for 3 min. A) Magnitudes of changes in tetanic $[Ca^{2+}]_i$ for individual glibenclamide- and verapamil-exposed wild type fibres. B) Group V1 consisted of fibres that had the smallest and slowest decrease in tetanic $[Ca^{2+}]_i$ (top 3 fibres in A). C) Group K2 consisted of the remaining fibres that had faster decreases in tetanic $[Ca^{2+}]_i$ (bottom 9 fibres in A). This approach was used because the differences between fibers were more gradual compared to the control and glibenclamide conditions. For this reason, statistical differences were not calculated.

Figure 3.17

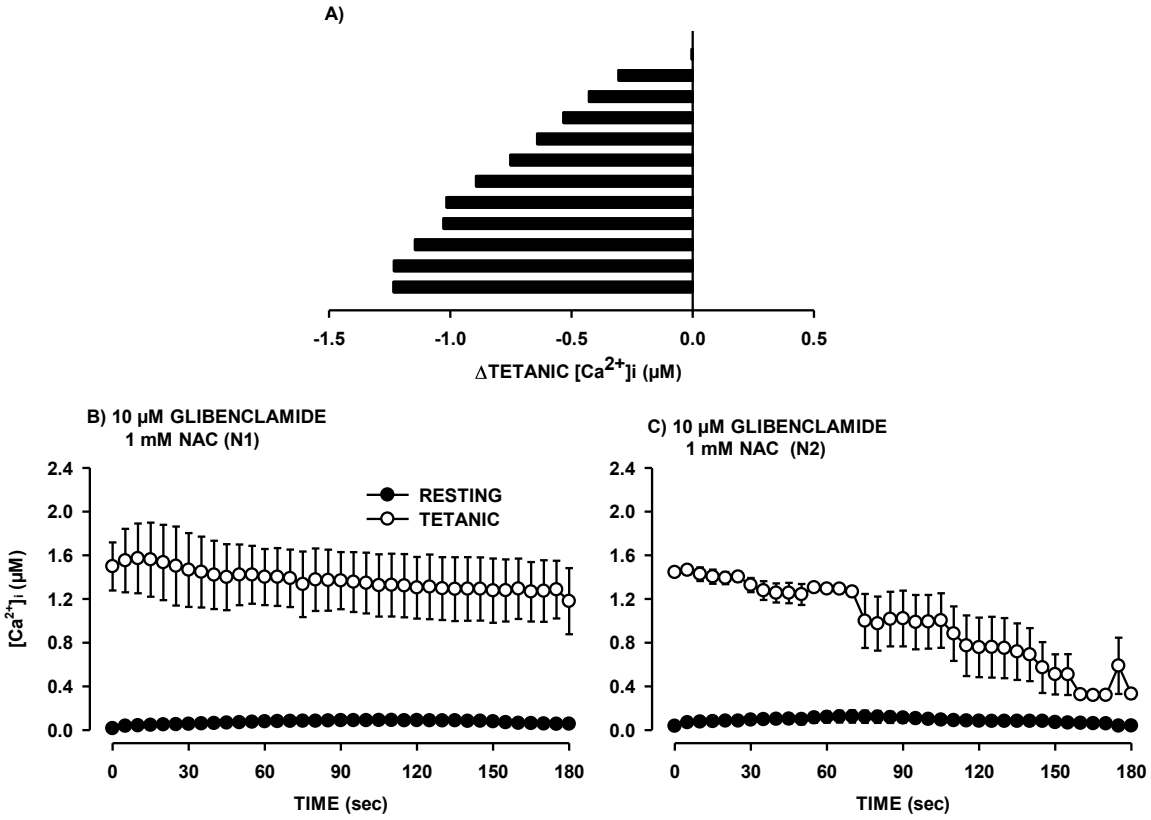

Figure 3.17. Fatigue kinetics of individual wild type FDB single fibres exposed to glibenclamide and NAC. Fatigue was elicited with one 200 ms long tetanic contraction (100 Hz) every sec for 3 min. A) Magnitudes of changes in tetanic $[Ca^{2+}]_i$ for individual glibenclamide- and NAC-exposed wild type fibres. B) Group N1 consisted of fibres that had little changes in tetanic $[Ca^{2+}]_i$ (top 4 fibres in A). C) Group N2 consisted of fibres that had larger loss in tetanic $[Ca^{2+}]_i$ (bottom 7 fibres). As explained in Fig. 3.16, no statistical analyses were carried out for these data.

CHAPTER 4

DISCUSSION

The major findings of this study were: (1) a collagenase digestion in MEM yielded fibres with better morphology (straight fibre appearance with clearly visible A and I bands) and better contractility (lower contraction threshold before and after fatigue, more fibres contracting); (2) the absence of FBS in the culture medium during the collagenase digestion resulted in most fibres being damaged or supercontracted; (3) the addition 0.2% FBS (v/v) to the superfusing physiological solution during experiments significantly improved fibre morphology and contractility; (4) a rapid increase in temperature from 25°C to 37°C had adverse effects on contractility. A gradual increase caused no such effects; (5) when single FDB fibres were isolated using collagenase in MEM with 10% FBS (v/v) and tested in physiological solution with 0.2% FBS (v/v) on the day of dissociation, they maintained stable morphology and contractility for at least three hours; (6) contrary to a previous study, differences in unstimulated and tetanic $[Ca^{2+}]_i$ kinetics during fatigue were observed when comparing glibenclamide-exposed wild type fibres and Kir6.2$^{-/-}$ fibres; (7) verapamil reduced the elevated unstimulated and tetanic $[Ca^{2+}]_i$ in glibenclamide-exposed FDB muscle fibres during fatigue; (8) NAC had similar effects to those of verapamil.

Single FDB fibres as a muscle preparation to study fatigue

Importance of MEM, DMEM and FBS

Mechanical dissection of single fibres is a common method for the study of muscle fatigue in terms of myoplasmic $[Ca^{2+}]_i$ and force (Moopanar & Allen, 2006). While this

method gives viable fibres, it requires a three hour dissection limiting the number of fibres one can test in one day. For E_m to be measured with microelectrodes, a long-term objective in this laboratory, a major problem arises because it is a delicate procedure that often leads to membrane damage and premature fibre death; i.e. a large amount of time can be consumed in dissecting single fibres instead of E_m measurement. While separating single fibres following a collagenase digestion also takes three to four hours of preparation, it yields hundreds of fibres. This improves the capacity to do E_m measurements as well as allowing for more selection of good, viable fibres to study. It also allows for immediate access to replacement fibres should a fibre become damaged or lost during an experiment.

Most studies that have used a collagenase digestion to separate fibres measured ion channel activity under membrane patch clamp. Very few used such fibres to study E_m, Ca^{2+}, or contractility. More importantly, since the very first publication by Bekoff (Bekoff & Betz, 1977), little has been done in testing and documenting the viability of these fibres; so one aim of this study was to optimize the isolation of single fibres via collagenase digestion.

In regard to the culture medium for the digestion, studies have used both MEM (Pye, 2007) and DMEM (Lindinger *et al.*, 2011). In this study, the use of MEM resulted in the largest number of fibres with good morphology and contractility. This result was surprising because DMEM contains a higher glucose concentration and a greater variety of nutrients than MEM (Appendix 1). The difference in effects cannot be explained from the results of this study. FBS was also important. The complete absence of FBS during the digestion resulted in most fibres being damaged or supercontracted at the end of the digestion period. At the time of this study, it was general practice to use 10% FBS during a collagenase digestion in MEM. Elevated concentrations of FBS in the physiological solution, such as

10%, presented an obstacle, as higher FBS content caused the formation of bubbles and foam during the O_2:CO_2 bubbling of the physiological solution. So, as a first test, 0.2% (v/v) FBS was used. The presence of 0.2% (v/v) FBS in the superfusing physiological solution during measurements also improved the contraction thresholds for fibres, as well as enhancing the recovery from fatigue. Recent E_m studies have shown that the optimal FBS concentration in the physiological solution is between 0.2% and 1% FBS (Hesse and Renaud, unpublished results).

The protective effect of FBS on single fibres during fatigue cannot be fully explained by the results of this study. It is known that addition of serum to cells in culture activates a transcription factor named serum response factor (SRF). SRF acts on numerous genes including skeletal and cardiac α-actin (Miwa & Kedes, 1987;Muscat *et al.*, 1988), α- and β-myosin heavy chain (Molkentin *et al.*, 1996;Huang *et al.*, 1997), troponin (Wang *et al.*, 1994), tropomyosin (Toutant *et al.*, 1994), creatine kinase (Vincent *et al.*, 1993), and SERCA (involved in cellular Ca^{2+} modulation) (Baker *et al.*, 1998). Since SRF regulates transcription when cells are stressed (Avantaggiati *et al.*, 1993), it is likely that FBS may act via SRF to improve the survival during the isolation protocol.

The final protocol, as determined by this study, involves a three hour collagenase digestion of FDB muscles in MEM culture medium containing 10% FBS. The fibres are then placed on glass coverslips covered with a thin coat of Matrigel™. After mounting the coverslip into a chamber, single FDB fibres are superfused with physiological solution containing 0.2% (v/v) FBS.

Viability of single FDB fibres after a collagenase treatment

After developing the protocol, it was important to determine the viability of fibres. One important factor in the contractility of these fibres was the speed at which fibres were re-heated from room temperature to 37°C, after placing the cover slip in the chamber and the latter in the microscope. It proved important to ensure a gradual re-heating of fibres from room temperature. Using progressive heating to 37°C yielded fibres that were stable for at least three hours if studied on the same day as the preparation. The next question is whether these fibres have contractile characteristics in line with expectations derived from fibres in whole muscle preparations. For this, three characteristics of single fibres were studied and compared to whole muscle: (1) contraction threshold; (2) stimulation frequency – sarcomere shortening relationship; and (3) recovery following fatigue. Finally, characteristics of the single fibres isolated by the current protocol were compared to mechanically dissected single fibre preparation, as well as compared to single fibres isolated by the collagenase digestion method, used previously in this laboratory.

Tetanic contractions were triggered in single FDB fibres with stimulation strength as low as two V, and the number of contracting fibres increased as stimulation strength was increased, reaching a maximum by 10 V. FDB bundles generate small force at stimulus strength of two V. The amount of force increases as stimulation strength increases reaching a maximum at eight V (Cifelli *et al.*, 2008); the increase in force being due to more fibres being recruited at higher stimulation strength. Single fibres prepared in a collagenase digestion have similar contraction threshold to that observed in mechanically dissected FDB fibres or FDB bundles.

Force of whole muscle is also a function of stimulation frequency increasing in magnitude from 0 Hz to 150 Hz (Place *et al.*, 2009). The increase in force is in part because fibres have more time to generate force and because of higher tetanic $[Ca^{2+}]_i$. More importantly, testing at 37°C shifts the force – frequency curve to higher frequencies because, at 37°C, Ca^{2+} ATPases pump Ca^{2+} more rapidly into the SR; i.e. at a given frequency, tetanic $[Ca^{2+}]_i$ is more elevated at lower temperature. While force was not measured, extent of shortening was also a function of frequency. This is because as the sarcomere shortens, the thin filaments come into contact and the Z lines touch the thick filaments, resulting in an increase in resistance that needs to be overcome by an increase in force production. The higher frequency results in higher tetanic $[Ca^{2+}]_i$ and greater force production. The greater force produced then gives rise to more shortening. The shift in shortening – stimulation frequency relationship towards higher frequencies as a result of heating from 25°C to 37°C in single fibres is in agreement with a similar shift for the force – frequency relationship in whole muscle.

A hallmark of viable single fibre preparation for the study of fatigue is that they fully recover following fatigue, as is observed for whole muscle or mechanically isolated single fibres (Cifelli *et al.*, 2007). During fatigue, there is a decrease in the extent of shortening as force decreases, and a decrease in resting length as unstimulated $[Ca^{2+}]_i$ increases. The fibres obtained from the preparation used in this study fully recovered their capacity to shorten, as well as their original resting length within 10 min of recovery following fatigue.

FDB fibres isolated via collagenase digestion in MEM containing 10% FBS behaved similarly to mechanically dissected single FDB fibres in terms of $[Ca^{2+}]_i$ kinetics, contractility, and response to changes in stimulation frequency (Moopanar & Allen, 2006).

Fibres isolated in this study were compared to fibres isolated in previous studies. The fibres in this study displayed better morphology and contractility properties to others obtained by similar means (Bourassa, 2007). In wild type control single FDB fibres, fatigue kinetics were similar between single fibres prepared by Bourassa and this study. In fibres with reduced K_{ATP} channel activity, due to exposure to glibenclamide or isolated from a genetic knockout for Kir6.2 gene, in the Bourassa study, there were large increases in unstimulated and tetanic $[Ca^{2+}]_i$ observed with fibres often losing capacity to contract before the end of the fatigue protocol, often due to supercontraction of fibres. In the current study, while $[Ca^{2+}]_i$ transients and kinetics were similar to those of Bourassa, there were less instances of fibres skipping contractions or stopping contracting completely before the end of a fatigue protocol. Furthermore, there were no supercontractions observed due to fatigue. This improvement is possibly due to the exclusive study of fibres on the same day of dissection and isolation (day 0), in the current study, compared to testing on the day following dissection and isolation (day 1), in the Bourassa study (Fig. 3.7-8). The reduced effect of fatigue on fibres in this study compared to those of Bourassa are likely due to the addition of 0.2% (v/v) FBS to the superfusing physiological solution. Without FBS in the physiological solution, effects of fatigue were more severe.

Overall, isolation of FDB single fibres following a collagenase digestion provides a large number of single fibres with normal morphology and contractility. In the future, it would be very interesting to repeat the measurements done in this study and determine the fibre types of fibres, to gain insight into the effects of fibre type on characteristics and behaviour during fatigue.

Role of K_{ATP} channel, L-type Ca^{2+} channel and ROS during fatigue

Unstimulated and tetanic $[Ca^{2+}]_i$: wild type control fibres

Major differences in the changes in unstimulated and tetanic $[Ca^{2+}]_i$ during fatigue at 37°C were observed among wild type FDB fibres tested under control conditions. These control fibres ranged from the most fatigue resistant fibres, for which post-fatigue tetanic $[Ca^{2+}]_i$ varied from 0.11-0.51 μM above pre-fatigue levels, to the least fatigue resistant fibres, for which tetanic $[Ca^{2+}]_i$ decreased by 0.09-1.40 μM during fatigue. FDB muscles primarily express myosin type I, IIA and IIX fibres (Banas *et al.*, 2011). However, FDB fibres expressing myosin type I also co-express either myosin type IIA or IIX, giving rise to type I-IIA (6%) and I-IIX (8%) fibres, as opposed to pure type I fibres. The most common fibre types in FDB are types IIA-IIX (32%), IIA (19%) and IIX (21%). It is suggested that the most fatigue resistant wild type FDB fibres observed in this study are the type I-IIA (and perhaps I-IIX) fibres, because fibres expressing myosin type I are slow-twitch fibres with low myosin ATPase activity and high oxidative capacity (Pellegrino *et al.*, 2003). It is also being suggested that the least fatigue resistant fibres are type IIX, because type IIX fibres are fast twitch fibres with high glycolytic capacity (and low oxidative capacity) (Pellegrino *et al.*, 2003). Type IIA and type IIA-IIX most likely make up the intermediately fatigue resistant fibres, since type IIA are fast twitch fibres with a high oxidative capacity.

In a previous study on fatigue at 25°C also using single FDB fibres, the time for the force to decrease by 70% was measured (Lannergren & Westerblad, 1991). Of a total of 26 fibres, that time ranged between four and seven min for 19 (73%) fibres while only three (12%) fibres had time exceeding 12 min, being highly fatigue resistant. It thus appears that

the differences in fatigue kinetics between fibres in this study are much greater than previously reported. There are two possible reasons for such differences. First, the stimulation protocols are different. In the Lannergren & Westerblad study, the time interval between contractions is initially 4 sec, and is reduced by 1 sec every two min until it reaches an interval of 1 sec between contractions. In this study, the time interval between contractions was maintained at 1 sec for the entire duration. However, most of the decrease in tetanic $[Ca^{2+}]_i$ and force in the Lannergren & Westerblad study starts when the interval between contractions becomes 1 sec. It is therefore unlikely that the differences between the two studies are mainly related to the difference in stimulation protocol.

Another basis for this difference is experimental temperature; being 37°C in this study and 25°C in the other. The depressive effects of acidic pH, inorganic phosphate, and K^+ are less significant at the near-physiological temperature of 37°C than they are at lower temperatures (Debold *et al.*, 2006;Westerblad *et al.*, 1997;Pedersen *et al.*, 2003). Also, metabolic demand is much higher at 37°C (Barclay, 2005), and performing experiments at this temperature would serve to better emphasize the differences in fatigue kinetics between highly glycolytic and highly oxidative fibres. Another consideration is that muscle temperature during exercise greatly exceeds 37°C (Fuller *et al.*, 1998;Gonzales-Alonso *et al.*, 1999). Interestingly, Cifelli et. al 2001 argued that studies on muscle fatigue should be carried out at 37°C.

Unstimulated and tetanic $[Ca^{2+}]_i$: contractile dysfunctions in K_{ATP} channel deficient FDB fibres

Blocking K_{ATP} channels with glibenclamide drastically alters fatigue kinetics in terms of tetanic $[Ca^{2+}]_i$, as previously reported (Cifelli *et al.*, 2007;Cifelli *et al.*, 2008). That is, the decrease in tetanic $[Ca^{2+}]_i$ and the increase in unstimulated $[Ca^{2+}]_i$ during fatigue were much greater than those of control fibres. Initial studies using EDL and soleus have reported similar fatigue kinetics between Kir6.2$^{-/-}$ and glibenclamide-exposed wild type muscles (Gong *et al.*, 2000;Gong *et al.*, 2003). However, three differences were observed when smaller muscle preparations were used (Cifelli *et al.*, 2007;Cifelli *et al.*, 2008). Firstly, the decreases in tetanic force of small FDB bundles during fatigue, while greater in K_{ATP} channel deficient muscles than in control, were smaller in Kir6.2$^{-/-}$ than in glibenclamide-exposed fibres. Secondly, the same situation was observed for the decreases in tetanic $[Ca^{2+}]_i$ in single FDB fibres. Furthermore, a sudden and drastic decrease in tetanic $[Ca^{2+}]_i$ occurred over a 10 sec period during fatigue, when glibenclamide was present in both wild type and Kir6.2$^{-/-}$ fibres; but this decrease was not observed in Kir6.2$^{-/-}$ fibres in the absence of glibenclamide. Thirdly, Kir6.2$^{-/-}$ FDB muscle had a reduced capacity to recover force during fatigue when glibenclamide was present, compared to when it was not.

In this study, we still observed greater decreases in tetanic $[Ca^{2+}]_i$ in K_{ATP} channel deficient fibres compared to control, but the differences between Kir6.2$^{-/-}$ and glibenclamide-exposed wild type fibres were much greater than what was observed in Cifelli's studies. While a direct comparison in fatigue kinetics, in which force is measured in FDB bundles and tetanic $[Ca^{2+}]_i$ in single fibres, must be done with caution, the fact remains that the results of this study better explain the differences in the force decreases observed during fatigue

between the two models of K_{ATP} channel deficiency. Perhaps, in this study, the single fibre preparation was much better than in Cifelli's studies, because we carried out our measurements the same day fibres were prepared, as opposed to the following day. Another reason is that in this study the physiological solution contained 0.2% (v/v) FBS. These are two changes in protocol that significantly improved the viability of the single fibre preparation. Taken together, this suggests that the decrease in tetanic $[Ca^{2+}]_i$ and force during fatigue is enhanced in the absence of K_{ATP} channel activity, but to a larger degree when glibenclamide is used to block K_{ATP} channels than when the channel activity is abolished by genetic means.

Glibenclamide-exposed wild type fibres had significantly larger increases in unstimulated $[Ca^{2+}]_i$ during fatigue than did control fibres, as previously reported (Cifelli *et al.*, 2007;Cifelli *et al.*, 2008). Such increases in tetanic $[Ca^{2+}]_i$ also explain the large increases in unstimulated force observed during fatigue in glibenclamide-exposed FDB bundles. Contrary to the previous studies, we found no large increases in unstimulated $[Ca^{2+}]_i$ in Kir6.2$^{-/-}$ fibres. In fact, they were not different from those of wild type control fibres. At first, this seems to be in agreement with the above conclusion regarding tetanic $[Ca^{2+}]_i$, i.e. that the extent of the contractile dysfunctions in K_{ATP} channel deficient fibres is less in Kir6.2$^{-/-}$ than it is in glibenclamide-exposed fibres. However, it does not explain the fact that the increase in unstimulated force during fatigue in Kir6.2$^{-/-}$ FDB bundles is as high as it is in glibenclamide-exposed FDB bundles.

One possibility for these discrepancies originates from a fundamental difference between bundle and single fibre preparation. As discussed by Cifelli et al., FDB bundles, while very small, still are large enough to result in a central hypoxic core during fatigue, at

37°C. With single fibres, this problem is eliminated, and perhaps the large increases in unstimulated $[Ca^{2+}]_i$ and force are greater when O_2 availability is impaired. In support of this hypothesis is the fact that severe fibre damage occurs during treadmill running in Kir6.2$^{-/-}$ mice (Thabet *et al.*, 2005). This is likely due to a lack of channel activity that does not only occur in skeletal muscle, but also in cardiac and diaphragm muscles, for which fibre damage has also been reported; the net effect being a reduced blood flow and O_2 delivery to limb muscles.

Another important consideration is that the use of glibenclamide acutely abolishes K_{ATP} channel activity, whereas Kir6.2$^{-/-}$ represents a chronic loss of K_{ATP} channel activity; i.e., Kir6.2$^{-/-}$ muscles may develop some compensatory mechanisms that allow them to better face a fatigue challenge, as long as there is a good O_2 delivery, but fail if the fatigue challenge is associated with decreases in O_2 availability.

A third possibility is glibenclamide specificity. There is currently no evidence that glibenclamide affects other ion channels than the K_{ATP} channel, when muscles are unfatigued and at rest (Pedersen *et al.*, 2009). However, a recent study has demonstrated large increases in membrane conductance when muscles are repetitively stimulated. Using 9-AC, a ClC-1 Cl^- channel blocker, it was shown that ≈ 76% of the increased membrane conductance was due to an activation of the ClC-1 Cl^- channels, and such an increases is expected to also increase the K^+-induced force depression (i.e., fatigue). The remaining increase in membrane conductance of ≈ 24% is then believed to be related to an activation of K^+ channels. However, the addition of glibenclamide resulted in a decrease in membrane conductance greatly exceeding 24% (Pedersen *et al.*, 2009). While this suggests that part of the increase in membrane conductance is related to an activation of K_{ATP} channels, which reduces action

potential amplitude also causing fatigue (Gong *et al.*, 2003), it raises the question as to whether glibenclamide or 9-AC remains specific to their ion channels when fibres are in a fatigued state. Considering the discussion above, and that contractile dysfunctions are greater when glibenclamide is present, we suggest that perhaps glibenclamide also affects ClC-1 channels, at least when fibres are in a fatigued state. This then implies that an increase in both K_{ATP} and ClC-1 channel activity is important in preventing fibre damage and contractile dysfunctions during fatigue. Further studies will be necessary to determine if glibenclamide does indeed block ClC-1 channel activity in fatigued fibres.

Not all fibres depend on the K_{ATP} channel for myoprotection

An important aspect of our findings is the difference in fatigue kinetics between fibres. That is, not all fibres were affected by a deficiency in K_{ATP} channel activity, whether caused by an exposure to glibenclamide or by gene knockout. Some fibres with reduced K_{ATP} channel activity had a fatigue resistance comparable to the most fatigue resistant fibres under control conditions, displaying no net, or small (<15%) decreases in tetanic $[Ca^{2+}]_i$. While repetitive stimulation of EDL fibres eventually leads to large increases in K_{ATP} and ClC-1 channel activity, this is not the case in soleus muscle. The lack of any increase in activity is most likely because soleus expresses type I and IIA fibres. The high oxidative capacity of these fibres likely resulted in the stimulation protocol never having created the metabolic stress necessary for the activation of K_{ATP} channels. The same situation likely occurred in this study. The oxidative capacity of the most fatigue resistant fibres is probably elevated enough that the fatigue stimulation did not result in any major metabolic stress, and therefore no activation of K_{ATP} channels, resulting in no observable glibenclamide effect. A complete lack of K_{ATP} or ClC-1 channel activity is, however, unlikely, considering that in the

most fatigue resistant fibre, the increase in unstimulated $[Ca^{2+}]_i$ occurred within 10 sec to 163 μM, compared to 100 sec in control fibres; i.e., a small increase in K_{ATP} channel activity at the onset, as observed for an increase K^+ conductance in the Pedersen study, may be important for maintaining resting membrane potential, especially if there is a decrease in Cl^- conductance first.

This is in agreement with the fact that fibres expressing myosin type I have the lowest K_{ATP} channel content. Fibres expressing myosin type IIX are probably the most stressed metabolically, and one would expect larger activation of K_{ATP} and ClC-1 channels in these fibres, resulting in faster decrease in tetanic $[Ca^{2+}]_i$ in the presence of glibenclamide or in Kir6.2$^{-/-}$ fibres. This also agrees with the fact that fibres expressing myosin IIX have the largest K_{ATP} channel content among FDB fibres. Fibres expressing myosin type IIA would then be the fibres with intermediate fatigue resistance

The increase in unstimulated $[Ca^{2+}]_i$ may not be all related to opening of L-type Ca^{2+} channels

In 2007, Cifelli et al. demonstrated that reduced K_{ATP} channel activity in FDB bundles during fatigue resulted in large increases in unstimulated force due to a large increase in unstimulated $[Ca^{2+}]_i$. Then, in 2008, Cifelli et al. suggested that the K_{ATP} channel is crucial in preventing excessive Ca^{2+} influx through L-type Ca^{2+} channels. Their conclusion was based on the fact that many fibres depolarize to -30 mV during contraction, an E_m at which Ca^{2+} channels are active (Gramolini & Renaud, 1997;Baczko *et al.*, 2004). Finally, they showed that one μM verapamil, a known Ca^{2+} channel blocker (Gallant & Goettl, 1985) abolishes the

increase in unstimulated force that is developed between contractions in K_{ATP} channel deficient muscle.

In this study, there were no differences in mean unstimulated or mean tetanic $[Ca^{2+}]_i$ between wild type control fibres, and glibenclamide-exposed wild type fibres, before fatigue. During fatigue, however, there was a much larger increase in unstimualted $[Ca^{2+}]_i$ in glibenclamide-exposed fibres than there was in control fibres. Adding verapamil to the fibres that were also exposed to glibenclamide had the effect of abolishing this large increase in unstimulated $[Ca^{2+}]_i$ during fatigue. This study, therefore, supports Cifelli's suggestion that the increase in unstimulated $[Ca^{2+}]_i$ is due, at least partially, to an influx of Ca^{2+} through L-type Ca^{2+} channels during fatigue, in these fibres.

Cifelli et. al also showed that K_{ATP} deficient FDB bundles also had a more rapid rate of fatigue in addition to the elevated unstimulated force. In this study, there was a larger initial increase in tetanic $[Ca^{2+}]_i$ in glibenclamide-exposed fibres, followed by a more rapid and larger decrease than observed in control fibres, with more fibres losing capacity to contract or produce tetanic $[Ca^{2+}]_i$, than control fibres. Treating glibenclamide-exposed fibres with verapamil reduced the magnitude of the initial increase in tetanic $[Ca^{2+}]_i$, as well as the extent to which tetanic $[Ca^{2+}]_i$ was reduced during fatigue. Verapamil treatment also reduced the number of fibres that stopped contracting altogether. These results in line with expectations based on force recordings obtained in the Cifelli study.

In a recent study, evidence was provided that an overload of Ca^{2+} may not be entirely due to L-Type Ca^{2+} channels (Gariepy-Boudreault, 2010). The study showed that NAC, a ROS scavenger, also prevents the large increase in unstimulated force in the same way as

verapamil. The hypothesis in the current study was that "the increase in resting $[Ca^{2+}]_i$ during fatigue in K_{ATP} channel deficient muscles starts with an excess Ca^{2+} influx through L-type Ca^{2+} channels (Phase 1, Fig. 4.1), followed by an excess ROS production that causes a further increase in resting $[Ca^{2+}]_i$" (Phase 2, Fig. 4.1). For this to be correct, in fibres exposed to glibenclamide and NAC, there should be an initial increase in tetanic $[Ca^{2+}]_i$ with the added activation of L-type Ca^{2+} channels, but the increase would be expected to be between control and glibenclamide-exposed fibres because the increase related to ROS would not occur as the latter are scavenged by NAC. However, NAC had the effect of reducing unstimulated $[Ca^{2+}]_i$ and reducing the rate of fatigue; i.e., the data did not support the hypothesis. However, fibres concomitantly treated with glibenclamide and NAC did not experience the initial increase in tetanic $[Ca^{2+}]_i$, observed with fibres under control, glibenclamide or glibenclamide/verapamil conditions. This suggests that NAC somehow reduced Ca^{2+} release during contraction in single FDB fibres. The reduced tetanic Ca^{2+} may have reduce the Ca^{2+} that needed to be pumped back into the sarcoplasmic reticulum between contractions; and this may have been sufficient to prevent the expected rapid increase in unstimulated Ca^{2+} associated with an influx through L-type Ca^{2+} channels (Fig. 4.1).

Since ROS was not measured in this study, it is not possible to know whether the NAC effects involved a reduction in ROS production or some other effects of NAC. Future studies will be necessary to clarify this issue.

Conclusion

In conclusion, in this study, an improved protocol was developed for the isolation of viable FDB single fibres and application of these fibres for $[Ca^{2+}]_i$ and sarcomere shortening

measurements. K_{ATP} channel deficient FDB single fibres obtained by this method were then used to study unstimulated and tetanic $[Ca^{2+}]_i$ during fatigue. This study has provided evidence that not all fibres are K_{ATP} channel dependent, and that the genetic model for K_{ATP} channel deficiency may allow for compensatory mechanisms to develop, making the effects of reduced K_{ATP} channel less severe. This study confirms that blocking L-type Ca^{2+} channels with verapamil reduces the elevated unstimulated $[Ca^{2+}]_i$ during fatigue in K_{ATP} channel deficient FDB fibres which is responsible for the increase in unstimulated force in FDB muscle during fatigue. This study also found that NAC had similar effects to verapamil, suggesting a role of ROS. It is still possible that there are other factors that may be contributing to the elevated $[Ca^{2+}]_i$ levels observed during fatigue in K_{ATP} channel deficient FDB fibres, independent of L-type Ca^{2+} channels. Further studies will be necessary to fully elucidate the role of ROS.

Figure 4.1

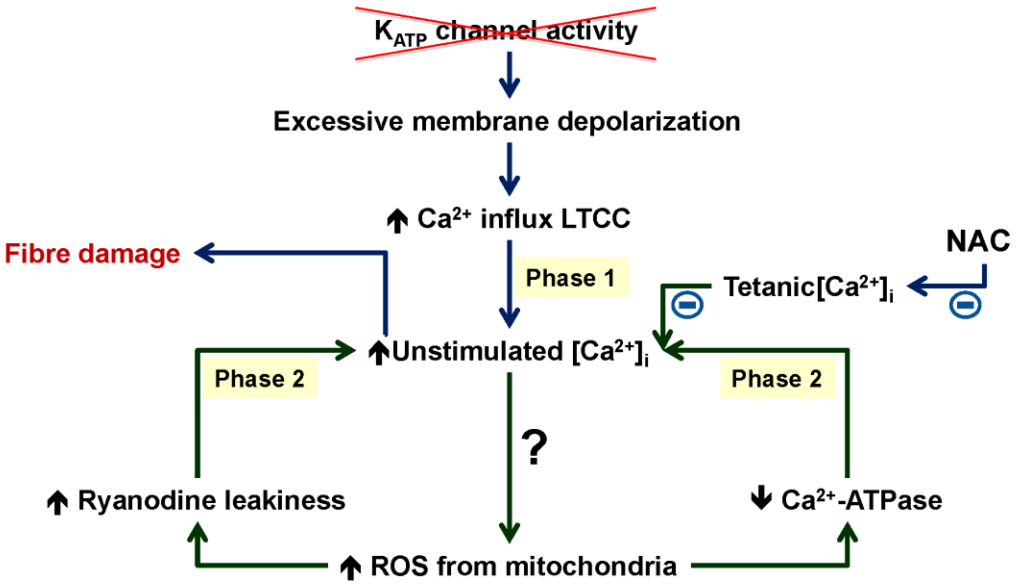

Figure 4.1. Factors causing the large increase in unstimulated $[Ca^{2+}]_i$ in K_{ATP} channel deficient FDB single fibres during fatigue. The first increase (Phase 1) starts with the activation of L-type Ca^{2+} channels as the sarcolemma depolarizes as reported by Cifelli et al. (2008). It was hypothesized that an increase in $[Ca^{2+}]_i$ then leads to increases in ROS levels causing further increases in $[Ca^{2+}]_i$. (Phase 2). However, NAC prevented large increases in tetanic $[Ca^{2+}]_i$ at the onset of the fatigue stimulation and may have helped preventing the large increase in unstimulated $[Ca^{2+}]_i$. Symbols: blue line, events for which there is evidence (Cifelli et al., 2008, this study); green line: events for which no evidence has so far been obtained.

APPENDIX 1

Table A.1: Minium essential medium (MEM) formulation (EAGLE *et al.*, 1959)

Components	Molecular Weight	Concentration (mg/L)	mM
Amino Acids			
L-Arginine hydrochloride	211	126	0.597
L-Cystine 2HCl	313	31	0.099
L-Glutamine	146	292	2
L-Histidine hydrochloride-H2O	210	42	0.2
L-Isoleucine	131	52	0.397
L-Leucine	131	52	0.397
L-Lysine hydrochloride	183	73	0.399
L-Methionine	149	15	0.101
L-Phenylalanine	165	32	0.194
L-Threonine	119	48	0.403
L-Tryptophan	204	10	0.049
L-Tyrosine disodium salt dihydrate	261	52	0.199
L-Valine	117	46	0.393
Vitamins			
Choline chloride	140	1	0.00714
D-Calcium pantothenate	477	1	0.0021
Folic Acid	441	1	0.00227
Niacinamide	122	1	0.0082
Pyridoxal hydrochloride	204	1	0.0049
Riboflavin	376	0.1	0.000266
Thiamine hydrochloride	337	1	0.00297
i-Inositol	180	2	0.0111
Inorganic Salts			
Calcium Chloride (CaCl2) (anhyd.)	111	200	1.8
Magnesium Sulfate (MgSO4) (anhyd.)	120	97.67	0.814
Potassium Chloride (KCl)	75	400	5.33
Sodium Bicarbonate (NaHCO3)	84	2200	26.19
Sodium Chloride (NaCl)	58	6800	117.24
Sodium Phosphate monobasic (NaH2PO4-H2O)	138	140	1.01
Other Components			
D-Glucose (Dextrose)	180	1000	5.56
Phenol Red	376.4	10	0.0266

Table A.2: Dulbeco's modified eagle medium (DMEM) formulation (DULBECCO & FREEMAN, 1959)

Components	Molecular Weight	Concentration (mg/L)	mM
Amino Acids			
Glycine	75	30	0.4
L-Arginine hydrochloride	211	84	0.398
L-Cystine 2HCl	313	63	0.201
L-Glutamine	146	584	4
L-Histidine hydrochloride-H2O	210	42	0.2
L-Isoleucine	131	105	0.802
L-Leucine	131	105	0.802
L-Lysine hydrochloride	183	146	0.798
L-Methionine	149	30	0.201
L-Phenylalanine	165	66	0.4
L-Serine	105	42	0.4
L-Threonine	119	95	0.798
L-Tryptophan	204	16	0.0784
L-Tyrosine disodium salt dihydrate	261	104	0.398
L-Valine	117	94	0.803
Vitamins			
Choline chloride	140	4	0.0286
D-Calcium pantothenate	477	4	0.00839
Folic Acid	441	4	0.00907
Niacinamide	122	4	0.0328
Pyridoxine hydrochloride	206	4	0.0194
Riboflavin	376	0.4	0.00106
Thiamine hydrochloride	337	4	0.0119
i-Inositol	180	7.2	0.04
Inorganic Salts			
Calcium Chloride (CaCl2) (anhyd.)	111	200	1.8
Ferric Nitrate (Fe(NO3)3"9H2O)	404	0.1	0.000248
Magnesium Sulfate (MgSO4) (anhyd.)	120	97.67	0.814
Potassium Chloride (KCl)	75	400	5.33
Sodium Bicarbonate (NaHCO3)	84	3700	44.05
Sodium Chloride (NaCl)	58	6400	110.34
Sodium Phosphate monobasic (NaH2PO4-H2O)	138	125	0.906
Other Components			
D-Glucose (Dextrose)	180	4500	25
Phenol Red	376.4	15	0.0399
Sodium Pyruvate	110	110	1

Reference List

Adrian RH, Chandler WK, & Hodgkin AL (1970). Voltage clamp experiments in striated muscle fibres. *J Physiol (Lond)* 208, 607-644.

Aguilar-Bryan L & Bryan J (1999). Molecular biology of adenosine triphosphate-sensitive potassium channels. *Endocrine Rev* 20, 101-135.

Allen DG, Lamb GD, & Westerblad H (2008). Skeletal muscle fatigue: cellular mechanisms. *Physiol Rev* 88, 287-332.

Allen DG, Lännergren J, & Westerblad H (1995). Muscle cell function during prolonged activity: cellular mechanisms of fatigue. *Exp Physiol* 80, 497-527.

Allen DG & Orchard CH (1987). Myocardial contractile function during ischemia and hypoxia. *Circ Res* 60, 153-168.

Antcliff JF, Haider S, Proks P, Sansom MSP, & Ashcroft FM (2005). Functional analysis of a structural model of the ATP-binding site of the KATP channel Kir6.2 subunit. *EMBO J* 24, 229-239.

Anzai K, Ogawa K, Ozawa T, & Yamamoto H (2000). Oxidative modification of ion channel activity of ryanodine receptor. *Antioxid Redox Signal* 2, 35-40.

Ashcroft FM & Kakei M (1989). ATP-sensitive K+ channels in rat pancreatic beta-cells: modulation by ATP and Mg2+ ions. *J Physiol* 416, 349-367.

Avantaggiati ML, Natoli G, Balsano C, Chirillo P, Artini M, De ME, Collepardo D, & Levrero M (1993). The hepatitis B virus (HBV) pX transactivates the c-fos promoter through multiple cis-acting elements. *Oncogene* 8, 1567-1574.

Babenko AP, Aguilar-Bryan L, & Bryan J (1998). A view of SUR/Kir6.X KATP channels. *Annu Rev Physiol* 60, 667-687.

Babenko AP & Bryan J (2003). Sur domains that associate with and gate KATP pores define a novel gatekeeper. *J Biol Chem* 278, 41577-41580.

Baczko I, Giles WR, & Light PE (2004). KATP channels reduces reoxygenation-induced Ca2+ overload in cardiac myocytes via modulation of the diastolic membrane potential. *Br J Pharmacol* 141, 1059-1067.

Baczko I, Jones L, McGuigan CF, Fox JEM, Gandhi M, Giles WR, Clanachan AS, & Light PE (2005). Plasma-membrane KATP channel-mediated cardioprotection involves posthypoxic reductions in calcium overload and contractile dysfunction: mechanistic insights into cardiopledia. *FASEB J Fj Express* 19, 980-982.

Baker DL, Dave V, Reed T, Misra S, & Periasamy M (1998). A novel E box/AT-rich element is required for muscle-specific expression of the sarcoplasmic reticulum Ca2+-ATPase (SERCA2) gene. *Nucleic Acids Res* 26, 1092-1098.

Balog EM, Thompson LV, & Fitts RH (1994). Role of sarcolemma action potentials and excitability in muscle fatigue. *J Appl Physiol* 76, 2157-2162.

Bangsbo J, Gollnick PD, Graham TE, Juel C, Kiens B, Mizuno M, & Saltin B (1990). Anaerobic energy production and O2 deficit-debt relationship during exhaustive exercise in humans. *J Physiol (Lond)* 422, 539-559.

Barclay CJ (2005). Modeling diffusive O2 supply to isolated preparations of mammalian skeletal and cardiac muscle. *J Muscle Res Cell Motil* 26, 225-235.

Barrett-Jolley R, Comtois A, Davies NW, Stanfield PR, & Standen NB (1996). Effect of adenosine and intracellular GTP on KATP channels of mammalian skeletal muscle. *J Membr Biol* 152, 111-116.

Bekoff A & Betz WJ (1977). Physiological properties of dissociated muscle fibres obtained from innervated and denervated adult muscle. *J Physiol (Lond)* 271, 25-40.

Blanchard EM & Solaro RJ (1984). Inhibition of the activation and troponin calcium binding of dog cardiac myofibrils by acidic pH. *Circ Res* 55, 382-391.

Bouclin R, Charbonneau E, & Renaud JM (1995). Na+ and K+ effect on contractility of frog sartorius muscle: implication for the mechanism of fatigue. *Am J Physiol* 268, C1528-C1536.

Boudreault L, Cifelli C, Bourassa F, Scott K, & Renaud JM (2010). Fatigue preconditioning increases fatigue resistance in mouse flexor digitorum brevis muscles with non-functioning KATP channels. *J Physiol (Lond)* 588, 4549-4562.

Bourassa F. KATP channel deficiency causes fiber damage and impairs Ca2+ release during fatigue in vitro. Master's Thesis. 2007.

Burton FL & Smith GL (1997). The effect of cromakalim on intracellular [Ca2+] in isolated rat skeletal muscle during fatigue and metabolic blockage. *Exp Physiol* 82, 469-483.

Cady EB, Jones DA, Lynn J, & Newham DJ (1989). Changes in force and intracellular metabolites during fatigue of human skeletal muscle. *J Physiol* 418, 311-325.

Cairns SP, Buller SJ, Loiselle DS, & Renaud JM (2003). Changes of action potentials and force at lowered [Na+]o in mouse skeletal muscle: implication for fatigue. *Am J Physiol Cell Physiol* 285, C1131-C1141.

Cairns SP, Flatman JA, & Clausen T (1995). Relation between extracellular [K+], membrane potential and contraction in rat soleus muscle: modulation by the Na+-K+ pump. *Pflugers Arch* 430, 909-915.

Campbell JD, Proks P, Lippiat JD, Sansom MS, & Ashcroft FM (2004). Identification of a functionally important negatively charged residue within the second catalytic site of the SUR1 nucleotide-binding domains. *Diabetes* 53 Suppl 3, S123-S127.

Champe PC, Harvey RA, & Ferrier DR. Biochemistry, 3rd ed. 1-534. 2005. Lippincott, Williams & Wilkins, New York.

Chaplin NL & Amberg GC (2012). Hydrogen peroxide mediates oxidant-dependent stimulation of arterial smooth muscle L-type calcium channels. *Am J Physiol Cell Physiol* 302, C1382-C1393.

Chin ER & Allen DG (1997). Effects of reduced muscle glycogen concentration on force, Ca2+ release and contractile protein function in intact mouse skeletal muscle. *J Physiol (Lond)* 498, 17-29.

Cifelli C, Boudreault L, Gong B, Bercier JP, & Renaud JM (2008). Contractile dysfunctions in KATP channel deficient mouse FDB during fatigue involve Ca2+ influx through L-type Ca2+ channels. *Exp Physiol* 93, 1126-1138.

Cifelli C, Bourassa F, Gariépy L, Banas K, Benkhalti M, & Renaud JM (2007). KATP channel deficiency in mouse FDB causes fiber damage and impairs Ca2+ release and force development during fatigue in vitro . *J Physiol (Lond)* 582, 843-857.

Clausen T (1996). The Na+, K+ pump in skeletal muscle: Quantification, regulation and functional significance. *Acta Physiol Scand* 156, 227-235.

Clement IV JP, Kunjilwar K, Gonzalez G, Schwanstecher M, Panten U, Aguilar-Bryan L, & Bryan J (1997). Association and stoichiometry of KATP channel subunits. *Neuron* 18, 827-838.

Cohen MV, Yang XM, & Downey JM (2008). Acidosis, oxygen, and interference with mitochondrial permeability transition pore formation in the early minutes of reperfusion are critical to postconditioning's success. *Basic Res Cardiol* 103, 464-471.

Cole WC, McPherson CD, & Sontag D (1991). ATP-regulated K+ channels protect the myocardium against ischemia/reperfusion damage. *Circ Res* 69, 571-581.

Craig TJ, Ashcroft FM, & Proks P (2008). How ATP inhibits the open K(ATP) channel. *J Gen Physiol* 132, 131-144.

Cui N, Li L, Wang X, Shi Y, Shi W, & Jiang C (2006). Elimination of allosteric modulation of myocardial KATP channels by ATP and protons in two Kir6.2 polymorphisms found in sudden cardiac death. *Physiol Genomics* 25, 105-115.

Davies NW (1990). Modulation of ATP-sensitive K+ channels in skeletal muscle by intracellular protons. *Nature* 343, 375-377.

Davies NW, Standen NB, & Stanfield PR (1992). The effect of intracellular pH on ATP-dependent potassium channels of frog skeletal muscle. *J Physiol (Lond)* 445, 549-568.

Dean M, Rzhetsky A, & Allikmets R (2001). The human ATP-binding cassette (ABC) transporter superfamily. *Genome Res* 11, 1156-1166.

Debold EP, Romatowski J, & Fitts RH (2006). The depressive effect of Pi on the force-pCa relationship in skinned single muscle fibers is temperature dependent. *Am J Physiol* 290, C1041-C1050.

Drain P, Li L, & Wang J (1998). KATP channel inhibition by ATP requires distinct functional domains of the cytoplasmic C terminus of the pore-forming subunit. *Proc Natl Acad Sci U S A* 95, 13953-13958.

DULBECCO R & FREEMAN G (1959). Plaque production by the polyoma virus. *Virology* 8, 396-397.

Dunne MJ & Petersen OH (1986). Intracellular ADP activates K+ channels that are inhibited by ATP in an insulin-secreting cell line. *FEBS Lett* 208, 59-62.

EAGLE H, PIEZ KA, FLEISCHMAN R, & OYAMA VI (1959). Protein turnover in mammaliar cell cultures. *J Biol Chem* 234, 592-597.

Faivre JF & Findlay I (1989). Effects of tolbutamide, glibenclamide and diazoxide upon action potentials recorded from rat ventricular muscle. *Biochim Biophys Acta* 984, 1-5.

Fong CN, Atwood HL, & Charlton MP (1986). Intracellular sodium activity at rest and after tetanic stimulation in muscles of normal and dystrophic (dy2j/dy2j)C57Bl/6J mice. *Exp Neurol* 93, 359-368.

Fryer MW, Owen VJ, Lamb GD, & Stephenson DG (1995). Effects of creatine phosphate and Pi on Ca2+ movements and tension development in rat skinned skeletal muscle fibres. *J Physiol (Lond)* 482, 123-140.

Fuller A, Carter RN, & Mitchell D (1998). Brain and abdominal temperatures at fatigue in rats exercising in the heat. *J Appl Physiol* 84, 877-883.

Gallant EM & Goettl VM (1985). Effects of calcium antagonists on mechanical responses of mammalian skeletal muscles. *Eur J Pharmacol* 117, 259-265.

Gariepy-Boudreault L. sKATP channels protect skeletal muscle against fibre damage during fatigue by preventing excessive increases in [Ca2+]i. PhD Thesis. 2010. University of Ottawa.

Gibbs CL (1987). Comparative muscle energetics and the cost of activation. *Proc Austr Physiol Pharmac Soc* 18, 115-123.

Gong B, Legault D, Miki T, Seino S, & Renaud JM (2003). KATP channels depress force by reducing action potential amplitude in mouse EDL and soleus. *Am J Physiol Cell Physiol* 285, C1464-C1474.

Gonzales-Alonso J, Teller C, Andersen SL, Jensen FB, Hyldig T, & Nielsen B (1999). Influence of body temperature on the development of fatigue during prolonged exercise in the heat. *J Appl Physiol* 86, 1032-1039.

Gramolini A & Renaud JM (1997). Blocking ATP-sensitive K+ channel during metabolic inhibition impairs muscle contractility. *Am J Physiol Cell Physiol* 41, C936-C946.

Gribble FM & Ashcroft FM (1999). Differential sensitivity of beta-cell and extrapancreatic K(ATP) channels to gliclazide. *Diabetologia* 42, 845-848.

Hamilton SL & Reid MB (2000). RyR1 modulation by oxidation and calmodulin. *Antioxid Redox Signal* 2, 41-45.

Hibino H, Inanobe A, Furutani K, Murakami S, Findlay I, & Kurachi Y (2010). Inwardly rectifying potassium channels: their structure, function, and physiological roles. *Physiol Rev* 90, 291-366.

Huang WY, Chen JJ, Shih N, & Liew CC (1997). Multiple muscle-specific regulatory elements are associated with a DNase I hypersensitive site of the cardiac beta-myosin heavy-chain gene. *Biochem J* 327 (Pt 2), 507-512.

Inagaki N, Gonoi T, & Seino S (1997). Subunit stochiometry of the ß-cell ATP-sensitive K+ channels. *FEBS Lett* 409, 232-236.

Inoue M, Sato EF, Nishikawa M, Park AM, Kira Y, Imada I, & Utsumi K (2003). Mitochondrial generation of reactive oxygen species and its role in aerobic life. *Curr Med Chem* 10, 2495-2505.

Ito H, Vereecke J, & Carmeliet E (1994). Mode of regulation by G protein of the ATP-sensitive K+ channel in guinea-pig ventricular membrane. *J Physiol (Lond)* 478, 101-108.

Jacobs I, Bar-Or O, Karlsson J, Dotan R, Tesch P, Kaiser P, & Inbar O (1982). Changes in muscle metabolites in females with 30-s exhaustive exercise. *Med Sci Sports Exerc* 14, 457-460.

Kakei M, Noma A, & Shibasaki T (1985). Properties of adenosine-triphosphate-regulated potassium channels in guinea-pig ventricular cells. *J Physiol (Lond)* 363, 441-462.

Kane GC, Behfar A, Dyer RB, O'Cochlain DF, Liu X-K, Hodgson DM, Reyes S, Miki T, Seino S, & Terzic A (2006). *KCNJ11* gene knockout of the Kir6.2 KATP channel causes maladaptive remodeling and heart failure in hypertension. *Human Molecular Genetics* 15, 2285-2297.

Karatzaferi C, de HA, van MW, & Sargeant AJ (2001). Metabolism changes in single human fibres during brief maximal exercise. *Exp Physiol* 86, 411-415.

Keung EC & Li Q (1991). Lactate activates ATP-sensitive potassium channels in guinea pig ventricular myocytes. *J Clin Invest* 88, 1772-1777.

Kirsch GE, Codina J, Birnbaumber L, & Brown AM (1990). Coupling of ATP-sensitive K+ channels to A1 receptors by G proteins in rat ventricular myocytes. *Am J Physiol* 259, H820-H826.

Kuo A, Gulbis JM, Antcliff JF, Rahman T, Lowe ED, Zimmer J, Cuthbertson J, Ashcroft FM, Ezaki T, & Doyle DA (2003). Crystal structure of the potassium channel KirBac1.1 in the closed state. *Science* 300, 1922-1926.

Lannergren J & Westerblad H (1986). Force and membrane potential during and after fatiguing, continuous high-frequency stimulation of single Xenopus muscle fibres. *Acta Physiol Scand* 128, 359-368.

Lannergren J & Westerblad H (1987). Action potential fatigue in single skeletal muscle fibres of Xenopus. *Acta Physiol Scand* 129, 311-318.

Lannergren J & Westerblad H (1991). Force decline due to fatigue and intracellular acidification in isolated fibres from mouse skeletal muscle. *J Physiol* 434, 307-322.

Larsson L, Edstrom L, Lindegren B, Gorza L, & Schiaffino S (1991). MHC composition and enzyme-histochemical and physiological properties of a novel fast-twitch motor unit type. *Am J Physiol* 261, C93-101.

Lee C & Okabe E (1995). Hydroxyl radical-mediated reduction of Ca(2+)-ATPase activity of masseter muscle sarcoplasmic reticulum. *Jpn J Pharmacol* 67, 21-28.

Li S, Zhengyan Z, Xielai Z, & Suhang L (2010). The effect of lead on intracellualr Ca2+ in mouse lymphocytes. *Toxic in Vitro* 22, 1815-1819.

Light PE & French RJ (1994). Glibenclamide selectively blocks ATP-sensitive K+ channels reconstituted from skeletal muscle. *Eur J Pharmacol* 259, 219-222.

Lindinger MI & Heigenhauser GJF (1991). The roles of ion fluxes in skeletal muscle fatigue. *Can J Physiol Pharmacol* 69, 246-253.

Lindinger MI, Leung M, Trajcevski KE, & Hawke TJ (2011). Volume regulation in mammalian skeletal muscle: the role of sodium-potassium-chloride cotransporters during exposure to hypertonic solutions. *J Physiol* 589, 2887-2899.

Liu GX, Derst C, Schlichthorl G, Heinen S, Seebohm G, Bruggemann A, Kummer W, Veh RW, Daut J, & Preisig-Muller R (2001). Comparison of cloned Kir2 channels with native inward rectifier K+ channels from guinea-pig cardiomyocytes. *J Physiol* 532, 115-126.

MacIntosh BR & Fletcher JR (2012). Reply to: reply to: the parabolic power-velocity relationship does apply to fatigued states. *Eur J Appl Physiol* 112, 1195-1196.

Matar W, Nosek TM, Wong D, & Renaud JM (2000). Pinacidil suppresses contractility and preserves energy but glibenclamide has no effect during fatigue in skeletal muscle. *Am J Physiol* 278, C404-C416.

McKenna MJ, Bangsbo J, & Renaud JM (2008). Muscle K+, Na+, and Cl– disturbances and Na+-K+ pump inactivation: implications for fatigue. *J Appl Physiol* 104, 288-295.

Merton PA (1954). Voluntary strength and fatigue. *J Physiol (Lond)* 123, 553-564.

Mikhailov MV, Campbell JD, de WH, Shimomura K, Zadek B, Collins RF, Sansom MS, Ford RC, & Ashcroft FM (2005). 3-D structural and functional characterization of the purified KATP channel complex Kir6.2-SUR1. *EMBO J* 24, 4166-4175.

Miki T, Iwanaga T, Nagashima K, Ihara Y, & Seino S (2001). Role of ATP-sensitive K+ channels in cell survival and differentiation in the endocrine pancreas. *Diabetes* 50 (suppl. 1), S48-S51.

Misler S, Falke LC, Gillis K, & McDaniel ML (1986). A metabolite-regulated potassium channel in rat pancreatic B cells. *Proc Natl Acad Sci U S A* 83, 7119-7123.

Miwa T & Kedes L (1987). Duplicated CArG box domains have positive and mutually dependent regulatory roles in expression of the human alpha-cardiac actin gene. *Mol Cell Biol* 7, 2803-2813.

Molkentin JD, Jobe SM, & Markham BE (1996). Alpha-myosin heavy chain gene regulation: delineation and characterization of the cardiac muscle-specific enhancer and muscle-specific promoter. *J Mol Cell Cardiol* 28, 1211-1225.

Moopanar TR & Allen DG (2005). Reactive oxygen species reduce myofibrillar Ca2+ sensitivity in fatiguing skeletal muscle at 37°C. *J Physiol (Lond)* 564, 189-199.

Moopanar TR & Allen DG (2006). The activity-induced reduction of myofibrillar Ca2+ sensitivity in mouse skeletal muscle is reversed by dithiothreitol. *J Physiol (Lond)* 571, 191-200.

Muscat GE, Gustafson TA, & Kedes L (1988). A common factor regulates skeletal and cardiac alpha-actin gene transcription in muscle. *Mol Cell Biol* 8, 4120-4133.

Nagaoka R, Yamashita S, Mizuno M, & Akaike N (1994). Intracellular Na+ and K+ shifts induced by contractile activities of rat skeletal muscles. *Comp Biochem Physiol [A]* 109, 957-965.

Nichols CG (2006). KATP channels as molecular sensors of cellular metabolism. *Nature* 440, 470-476.

Nielsen OB, Hilsted L, & Clausen T (1998). Excitation-induced force recovery in potassium-inhibited rat soleus muscle. *J Physiol* 512 (Pt 3), 819-829.

Noma A (1983). ATP-regulated K+ channels in cardiac muscle. *Nature* 305, 147-148.

Pedersen TH, Clausen T, & Nielsen OB (2003). Loss of force induced by high extracellular [K+] in rat muscle: effect of temperature, lactic acid and b2-agonist. *J Physiol (Lond)* 551, 277-286.

Pedersen TH, de Paoli F, & Nielsen OB (2005). Increased excitability of acidified skeletal muscle: role of chloride conductance. *J Gen Physiol* 125, 237-246.

Pedersen TH, de Paoli FV, Flatman JA, & Nielsen OB (2009). Regulation of CLC-1 and KATP channels in action potential-firing fast-twitch muscle fibers. *J Gen Physiol* 134, 309-322.

Pellegrino MA, Canepari M, Rossi R, D'Antona G, Reggiani C, & Bottinelli R (2003). Orthogous myosin isoforms and scalling of shortening velocity with body size in mouse, rat, rabbit and human muscles. *J Physiol (Lond)* 546, 677-689.

Place N, Yamada T, Zhang SJ, Westerblad H, & Bruton JD (2009). High temperature does not alter fatigability in intact mouse skeletal muscle fibres. *J Physiol (Lond)* 2009, 4717-4724.

Reimann F & Ashcroft FM (1999). Inwardly rectifying potassium channels. *Curr Opin Cell Biol* 11, 503-508.

Renaud JM (2002). Modulation of force development by Na+, K+, Na+ K+ pump and KATP channel during muscular activity. *Can J Appl Physiol* 27, 296-315.

Renaud JM & Mainwood GW (1985). The effects of pH on the kinetics of fatigue and recovery in frog sartorius muscle. *Can J Physiol Pharmacol* 63, 1435-1443.

Ronner P, Higgins TJ, & Kimmich GA (1991). Inhibition of ATP-sensitive K+ channels in pancreatic b-cells by nonsulfonylurea drug linogliride. *Diabetes* 40, 885-892.

Seino S (1999). ATP-sensitive potassium channels: a model of heteromultimeric potassium channel/receptor assemblies. *Annu Rev Physiol* 61, 637-662.

Senisterra GA, Huntley SA, Escaravage M, Sekhar KR, Freeman ML, Borrelli M, & Lepock JR (1997). Destabilization of the Ca2+-ATPase of sarcoplasmic reticulum by thiol-specific, heat shock inducers results in thermal denaturation at 37 degrees C. *Biochemistry* 36, 11002-11011.

Shyng SL, Ferrigni T, & Nichols CG (1997). Regulation of KATP channel activity by diazoxide and MgADP: Distinct functions of the two nucleotide binding folds of the sulfonylurea receptor. *J Gen Physiol* 110, 643-654.

Shyng SL & Nichols CG (1997). Octameric stoichiometry of the KATP channel complex. *J Gen Physiol* 110, 655-664.

Standen NB, Pettit AI, Davies NW, & Stanfield PR (1992). Activation of ATP-dependent K+ currents in intact skeletal muscle fibres by reduced intracellular pH. *Proc R Soc Lond B* 247, 195-198.

Standen NB, Quayle JM, Davies NW, Brayden JE, Huang Y, & Nelson MT (1989). Hyperpolarizing vasodilators activate ATP-sensitive K+ channels in arterial smooth muscle. *Science* 245, 177-180.

Stoller D, Pytel P, Katz S, Early JU, Collins K, Metcalfe J, Lang RM, & McNally EM (2009). Impaired exercise tolerance and skeletal muscle myopathy in sulfonylurea receptor-2 mutant mice. *Am J Physiol* 297, R1144-R1153.

Tanabe K, Tucker SJ, Matsuo M, Proks P, Ashcroft FM, Seino S, Amachi T, & Ueda K (1999). Direct photoaffinity labeling of the Kir6.2 subunit of the ATP-sensitive K+ channle by 8-azido-ATP. *J Biol Chem* 274, 3931-3933.

Tao X, Avalos JL, Chen J, & MacKinnon R (2009). Crystal structure of the eukaryotic strong inward-rectifier K+ channel Kir2.2 at 3.1 A resolution. *Science* 326, 1668-1674.

Thabet M, Miki T, Seino S, & Renaud JM (2005). Treadmill running causes significant damage in skeletal of muscle KATP channel deficient mice. *Physiol Gen* 22, 204-212.

Tortora GJ & Reynolds-Grabowski S. Principles of anatomy and physiology, 10th ed. 1-1248. 2003. Von Hoffman Press, New York.

Toutant M, Gauthier-Rouviere C, Fiszman MY, & Lemonnier M (1994). Promoter elements and transcriptional control of the chicken tropomyosin gene [corrected]. *Nucleic Acids Res* 22, 1838-1845.

Vasiliou V, Vasiliou K, & Nebert DW (2009). Human ATP-binding cassette (ABC) transporter family. *Hum Genomics* 3, 281-290.

Vercesi AE, Kowaltowski AJ, Grijalba MT, Meinicke AR, & Castilho RF (1997). The role of reactive oxygen species in mitochondrial permeability transition. *Biosci Rep* 17, 43-52.

Vincent CK, Gualberto A, Patel CV, & Walsh K (1993). Different regulatory sequences control creatine kinase-M gene expression in directly injected skeletal and cardiac muscle. *Mol Cell Biol* 13, 1264-1272.

Vollestad NK, Sejersted OM, Bahr R, Woods JJ, & Bigland-Ritchie B (1988). Motor drive and metabolic responses during repeated submaximal contractions in humans. *J Appl Physiol* 64, 1421-1427.

Wang G, Yeh HI, & Lin JJ (1994). Characterization of cis-regulating elements and trans-activating factors of the rat cardiac troponin T gene. *J Biol Chem* 269, 30595-30603.

Westerblad H & Allen DG (1991). Changes of myoplasmic calcium concentration during fatigue in single mouse muscle fibers. *J Gen Physiol* 98, 615-635.

Westerblad H & Allen DG (1993a). The contribution of [Ca2+]i to the slowing of relaxation in fatigued single fibres from mouse skeletal muscle. *J Physiol* 468, 729-740.

Westerblad H & Allen DG (1993b). The influence of intracellular pH on contraction, relaxation and [Ca2+]i in intact single fibres from mouse muscle. *J Physiol (Lond)* 466, 611-628.

Westerblad H, Bruton JD, & Lännergren J (1997). The effect of intracellular pH on contractile function of intact, single fibres of mouse muscle declines with increasing temperature. *J Physiol (Lond)* 500, 193-204.

Westerblad H, Dahlstedt AJ, & Lannergren J (1998). Mechanisms underlying reduced maximum shortening velocity during fatigue of intact, single fibres of mouse muscle. *J Physiol* 510 (Pt 1), 269-277.

Zhang L, Wehbi E, Miki T, Seino S, & Renaud JM (2002). KATP channel deficiency enhances basal glucose uptake in edl msucle but insulin responsiveness in soleus muscle. *Am J Physiol*.

Zingman LV, Hodgson DM, Bast PH, Kane GC, Perez-Terzic C, Gumina RJ, Pucar D, Bienengraeber M, Dzeja PP, Miki T, Seino S, Alekseev AE, & Trezic A (2002). Kir6.2 is required for adaptation to stress. *Proc Natl Acad Sci* 99, 13278-13283.